

The Hyper-K Underwater Electronics Assembly project

-

Letter of Intent

ETH Zurich, Institute for Particle physics and Astrophysics, Zurich, Switzerland

L. Botao, T. Dieminger, M. Franks, A. Gendotti, U. Kose, A. Rubbia, D. Sgalaberna, X. Zhao, J.
Wüthrich

Kamioka Observatory, Institute for Cosmic Ray Research (ICRR), U. of Tokyo, Japan

C. Bronner, Y. Hayato, K. Hiraide, K. Ieki, Y. Kataoka, Y. Noguchi, M. Shiozawa, Y. Takemoto

INFN Sezione di Bari, Bari, Italy

E. Radicioni

INFN Sezione di Napoli and Università Federico II di Napoli, Napoli, Italy

A. Boiano, G. De Rosa, A. Di Nitto, A. Langella, L. Lavitola, G. Ricciardi, G. Tortone

INFN Sezione di Padova and Università di Padova, Padova, Italy

G. Bortolato, G. Collazuol, D. D'Ago, M. Feltre, S. Levorato, A. Longhin, M. Mattiazzi, M. Pari,
F. Pupilli

INFN Sezione di Pisa and Università di Pisa, Pisa, Italy

G. Lamanna, L. Morescalchi, J. Pinzino, M. Sozzi

INFN Sezione di Roma and Università di Roma La Sapienza, Roma, Italy

F. Ameli, L. Ludovici, M. Rescigno

21 **IRFU, CEA, Université Paris-Saclay, Gif-sur-Yvette, France**

22 S. Bolognesi, D. Calvet, T. Daret, S. Emery, E.M. Gonzalez, S. Hassani, S. Joshi, G. Vasseur

23 **Jagiellonian University, Krakow, Poland**

24 K. Zięta

25 **King's College of London, London, United Kingdom**

26 F. Di Lodovico, S. Hayashida, K. Hayrapetyan, J. Migenda

27 **Laboratoire de Physique Nucléaire et de Hautes Energies (LPNHE), Sorbonne**
28 **Université, IN2P3-CNRS, Paris, France**

29 J. Dumarchez, G. Diaz Lopez, C. Giganti, M. Guigue, B. Popov, S. Russo, W. Saenz-Arevalo, M.
30 Zito

31 **Laboratoire Leprince-Ringuet (LLR), Ecole Polytechnique, IN2P3-CNRS, Palaiseau,**
32 **France**

33 L. Bernardi, O. Drapier, M. Buizza-Avanzini, F. Magniette, T. Mueller, P. Paganini, B. Quilain

34 **Lancaster University, Lancaster, United Kingdom**

35 T. Dealtry, L. Kormos, H.M. O'Keeffe

36 **Nicolaus Copernicus Astronomical Centre of the Polish Academy of Sciences, Poland**

37 M. Suchenek, M. Ziembicki

38 **Università di Salerno and INFN Gruppo Collegato di Salerno, Fisciano, Italy**

39 C. Bozza, L. Fusco

40 **Universitat Politècnica de València, Valencia, Spain**

41 F. Ballester Merelo, R. Esteve Bosch, A. Gómez Gambín, V. Herrero Bosch, F.J. Mora Mas, J.F.
42 Toledo Alarcón

43 **University of Geneva, Geneva, Switzerland**

44 F. Sánchez

45 **University of Glasgow, Glasgow, United Kingdom**

46 V.G.C. Lam, R.P. Litchfield, L.N. Machado, V. Mikola, S. Naik, D. Riley, F.J.P. Soler

47 **University of Silesia, Katowice, Poland**

48 A. Bubak, J. Holeczek, J. Kisiel

49 **University of Tokyo, Tokyo, Japan**

50 M. Yokoyama

51 **University of Warwick, Warwick, United Kingdom**

52 M. O'Flaherty, B. Richards

53 **Warsaw University of Technology, Warsaw, Poland**

54 A. Buchowicz, K. Dygnarowicz, G. Galiński, R. Kurjata, J. Marzec, W. Obreński, G. Pastuszek, A.

55 Rychter, K. Zaremba

56 **Yerevan Institute for Theoretical Physics and Modeling, Yerevan, Armenia**

57 A. Ioannisian

58
59 August 16, 2023

Contacts: davide.sgalaberna@cern.ch, marcin.ziembicki@pw.edu.pl

60 Contents

61	1 Executive summary	6
62	2 Introduction and Physics Case	7
63	2.1 The Hyper-Kamiokande experiment	9
64	3 The PMTs and the underwater electronics units	13
65	3.1 The electronics underwater unit	16
66	3.1.1 The digitizer	18
67	3.1.2 The Data Processing Board	20
68	3.1.3 The Low Voltage modules	22
69	3.1.4 The High Voltage modules	23
70	3.1.5 The time synchronization	25
71	3.1.6 The water-tight vessel	26
72	3.1.7 DAQ and Slow Control	29
73	3.2 Ongoing activities at CERN	30
74	3.2.1 Vertical Slice Tests	31
75	3.2.2 10-unit tests	32
76	3.3 The design and production schedule of the electronics underwater units	33
77	4 The Hyper-K Assembly project at CERN	36
78	4.1 Planned activities	36
79	4.1.1 Assembly of the underwater unit	37
80	4.1.2 Electronics tests	39
81	4.1.3 Pressurized tests	40
82	4.1.4 Long-term tests	41
83	4.2 Assembly project definition	42
84	4.2.1 Space for storage and activities	42
85	4.2.2 WA105 facility for long-term tests	45
86	4.2.3 Person power and technical personnel	45
87	4.2.4 Computing	47
88	4.3 Project milestones, time schedule and costs	47
89	4.3.1 Project schedule	47
90	4.3.2 Project costs	47
91	5 Conclusions and Outlook	49

93 **1 Executive summary**

94 Starting in 2027, the Hyper-Kamiokande experiment in Japan will search for leptonic CP violation in long-
95 baseline accelerator neutrino oscillations with a realistic potential of discovery within 3 to 10 years from the
96 start of the data taking depending on the value of the CP violating phase, to be measured with a resolution
97 better than 23° . The neutrino mass ordering will be determined with a significance better than four standard
98 deviations by combining data from accelerator and atmospheric neutrinos. Beyond the physics of neutrino
99 oscillations, Hyper-Kamiokande will achieve unprecedented sensitivities to the detection of proton decays
100 and supernova burst and relic neutrinos and will look for other types of astrophysical neutrinos, indirect
101 evidence of dark matter and sterile neutrinos.

102 A key contribution is given by European institutes, in particular to the far detector underwater electronics
103 system, that will allow to operate about 23,600 PMTs of the Hyper-Kamiokande water Cherenkov far detector,
104 of which 20,000 20-inch PMTs of the inner detector and 3,600 3-inch PMTs of the outer detector. About
105 900 electronics units will be installed underwater. Each one comprises two boards for the PMT signal
106 digitization, a data processing board, a high-voltage and a low-voltage module, all contained inside a stainless
107 steel water tight vessel.

108 In this Letter of Intent, we propose the SPSC to host at CERN under the program of the Neutrino
109 Platform a new project focused on the assembly, testing and shipment to Japan of the 900 underwater
110 electronics units. Such project is a common effort lead by the European institutes involved in Hyper-
111 Kamiokande, that would have easy access to the experimental facilities at CERN. After a preparatory phase,
112 the project will become fully operational at the beginning of 2025 for a duration of about 1.5 years. Space
113 for the storage of the sub-system components, assembled units and for the test and assembly activities will
114 be needed as well as technical expertise (mechanical engineer and technicians) and support for the shipment
115 to Japan. The project will be fully funded by the Hyper-Kamiokande collaboration, including the technical
116 personnel. CERN and the Neutrino Platform have been identified as the ideal framework to carry out such
117 project. Full support has been expressed by the leaders of the Neutrino Platform.

118 2 Introduction and Physics Case

119 Neutrino oscillations were discovered at the Super-Kamiokande (Super-K) experiment in Japan in 1998 with
120 atmospheric neutrinos [1]. **The existence of neutrino oscillations implies that at least two out of**
121 **three neutrinos have non-vanishing masses**, which is evidence of physics beyond the Standard Model
122 of particles. A few years later, the first hint of this phenomenon with solar neutrinos was found by combining
123 the Super-K and the Sudbury Neutrino Observatory (SNO) experiment data [2], and confirmed by the SNO
124 experiment [3]. Then, neutrino oscillations have been measured at KamLAND with reactor anti-neutrinos
125 [4] and, finally, at K2K, the first neutrino accelerator experiment in Japan [5].

126 The field steadily advanced in the last twenty-five years, getting very close to the completion of the 3-
127 flavor neutrino oscillation framework, described by the Pontecorvo-Maki-Nakagawa-Sakata (PMNS) mixing
128 matrix [6], lastly with the measurement of a non-zero θ_{13} angle by T2K [7, 8, 9] and Daya-Bay [10], as well
129 as the precise measurement of the neutrino eigenstate mass squared difference, Δm_{32}^2 and Δm_{21}^2 . There
130 remain only two undefined parameters: the neutrino mass ordering (MO), i.e. the sign of the neutrino
131 mass splitting Δm_{32}^2 , that could be measured with a precision better than three standard deviations by
132 different experiments, including NOvA [11], currently running, and JUNO [12], under construction, and,
133 in the future, with a significance better than five standard deviations by the DUNE experiment [13]; the
134 leptonic CP violating phase (δ_{CP}) that, if different from 0 and 180° , would make the appearance oscillation
135 probability different for neutrinos ($\nu_\mu \rightarrow \nu_e$) and antineutrinos ($\bar{\nu}_\mu \rightarrow \bar{\nu}_e$), hence, the laws of physics different
136 between particles and antiparticles. While the determination of the MO is a very important input for the
137 understanding of the nature of the neutrino mass, either Dirac or Majorana [6], CP violation is a necessary
138 ingredient for the understanding of the large imbalance between matter and antimatter in the Universe.
139 The precise measurement of δ_{CP} becomes even more important if one considers that the CP asymmetry in
140 the quark sector is too small to generate such imbalance. Moreover, the fact that the measured value of
141 neutrino mixing angle θ_{13} is relatively large has opened the door to the possible existence of a large leptonic
142 CP asymmetry, that may have initiated a process, called leptogenesis [14], potentially responsible for the
143 matter-antimatter imbalance generated after the Big Bang.

144 At the forefront in the field is the neutrino physics program in Japan, currently active with the Super-
145 Kamiokande (Super-K) and Tokai-to-Kamioka (T2K) experiments. Solar, atmospheric and supernova neu-
146 trino studies are conducted with Super-K as well as proton decay searches. Recently, Super-K was upgraded
147 by loading water with gadolinium (Gd) to improve the sensitivity to the supernova relic neutrinos. At T2K,
148 searches for CP violation in neutrino oscillations are performed by relying on the precise measurement of
149 the $\nu_\mu \rightarrow \nu_e$ and $\bar{\nu}_\mu \rightarrow \bar{\nu}_e$ transitions, to find the evidence for a difference in the respective oscillation prob-
150 abilities. It consists of measuring the number of ν_e ($\bar{\nu}_e$) interactions as a function of the neutrino energy
151 where the maximum of the oscillation probability occurs, far away from where neutrinos are produced, and

152 comparing it with the one predicted before neutrinos have oscillated. T2K deploys a “near detector” (ND),
153 a few hundred meters away from the neutrino production point, and Super-Kamiokande as “far detector”
154 (FD), 295 km away. Whilst the ND allows constraining the systematic uncertainties related to the neutrino
155 cross-section and flux, the role of the FD is to collect a large amount of neutrino interactions to measure
156 the oscillation probability with low statistical uncertainties. T2K has recently reported the first indication
157 of CP violation in the neutrino sector [15, 16] and is currently leading the field, with a projected sensitivity
158 to CP violation up to three standard deviations by 2027.

159 **The staged Japanese program ensures high quality physics results in the short term with**
160 **the upgraded T2K (beam and ND) and the upgraded Super-K (Super-K Gd) and, in the**
161 **medium/long term, with the upcoming Hyper-Kamiokande (Hyper-K) experiment [17, 18].**
162 Hyper-K will adopt the same concept as a combination of T2K and Super-K. The higher intensity neutrino
163 beam (up to 1.3 MW) and the 258 kton far detector, with a eight times larger fiducial mass than Super-K,
164 will provide a **realistic potential of discovering the leptonic CP violation (CPV) in a few to ten**
165 **years after the start of the accelerator neutrino data taking** and measuring δ_{CP} with a resolution of
166 $7 - 23^\circ$ depending on its value. Moreover, by combining data from accelerator and atmospheric neutrinos,
167 **the MO can be determined with a significance better than four standard deviations.**

168 Beyond accelerator physics, Hyper-K will have the world-leading sensitivity for several of the proton
169 decay modes, which may bring to the experimental proof of the Grand-Unified Theory (GUT).

170 On the global level, Hyper-K has been approved by the Japan’s Ministry of Education, Culture, Sports,
171 Science and Technology (MEXT) in 2020. The CERN European Strategy for Particle Physics 2020 (ESPP)
172 has classified the long baseline neutrino program as one of the major scientific objectives. For instance, the
173 CERN Neutrino Platform is involved in the neutrino Japanese program in the T2K experiment with the
174 upgrade of its magnetised near detector (ND280). The project NP07 was approved by the CERN SPSC to
175 provide technical support, logistic and direct contributions important for the realisation of the novel plastic
176 scintillator based neutrino active target (SuperFGD) and the two time projection chambers (TPC) [19]. The
177 NP07 project is ongoing and close to be completed.

178 **In this Letter of Intent (LoI), the Hyper-K collaboration proposes to the SPSC a new project**
179 **to be hosted at CERN under the Neutrino Platform program. The goal is the realisation of**
180 **the Hyper-K FD to start collecting accelerator neutrino data in 2027 Japanese Fiscal Year**
181 **(JFY). In particular, the project will focus on the validation, testing, assembly and shipment**
182 **to the experimental site in Japan of about 900 underwater electronics units that will allow the**
183 **operation of approximately 23,600 photomultiplier tubes (PMTs).**

184 2.1 The Hyper-Kamiokande experiment

185 In order to definitively discover CPV, Hyper-K will use the same 295 km baseline as T2K but will have a
186 larger FD fiducial mass and a higher neutrino beam intensity.

187 A major upgrade of the J-PARC proton accelerator, just completed, will allow to constantly increase the
188 neutrino beam intensity year after year, reaching 1.2 MW in 2027 and a maximum power of 1.3 MW in 2028,
189 higher by more than a factor two with respect to before the upgrade.

190 The higher beam intensity will be accompanied by a new water-Cherenkov far detector of 258 kton,
191 whose fiducial mass will be more than eight times larger than the Super-K one, making it the largest water
192 pool under the ground ever built in the world. The FD is a 68 m diameter and 71 m high cylindrical-
193 shape water tank detector filled with 258,000 metric tons of ultrapure water, currently in preparation at the
194 Kamioka facility in Japan. The Cherenkov light is read out by photomultiplier tubes (PMT). The detector
195 is divided into two optically-separated parts: the “Inner Detector” (ID) instrumented with about 20,000 20-
196 inch PMTs, as the main active volume which provides the time of the reconstructed neutrino interaction
197 vertex, the energy loss by charged particles, and their momentum. It will be surrounded by the Cherenkov
198 “Outer Detector” (OD), the external shell of the water tank instrumented with 3,600 outward looking 3-inch
199 PMTs, and act as a veto against incoming particles, like cosmic rays.

200 The ID will have a more performing photodetection system compared to Super-K. It will comprise two
201 types of photosensors: 20-inch diameter PMTs and multi-PMTs. About 20,000 20-inch PMTs, with the same
202 size as the Super-K one but a two times higher photodetection efficiency (PDE), will cover about 20% of
203 detector surface. The 1.5 ns time resolution, a factor two better than the one of the Super-K PMT, and
204 a comparable dark count rate (4 kHz) will provide an improved reconstruction of the neutrino interaction
205 event from the detected Cherenkov radiation [20]. In the ID there will be also 800 multi-PMTs, which are
206 composite sensors composed of nineteen 3-inch PMTs. Compared to the 20-inch PMTs, they will profit from
207 a finer granularity, hence a more precise reconstruction of the particle direction as well as an even lower time
208 resolution (1.3 ns). Being complementary to the 20-inch PMT, the multi-PMT will also allow to reduce the
209 detector systematic uncertainties. The OD will surround the ID and will consist of approximately 3,600 3-
210 inch diameter PMTs coupled with wavelength shifting plates to increase the total light yield. A simulation
211 of a muon and an electron in the Hyper-K FD is shown in Fig. 1.

212 Despite the much bigger volume and mass, the reconstruction performance for high energy events at
213 Hyper-K exceeds that of Super-K. This can be understood as a combination of higher light collection by
214 the photosensors and better timing resolution from the larger number of photosensors. Compared to Super-
215 K, the momentum resolution for electrons improves by 30% to 50% and for muons by 50%. The muon and
216 electron classification is comparable between Hyper-K and Super-K. The direction and the position resolution
217 is comparable to that of Super-K while significant improvements are seen in the particle identification of

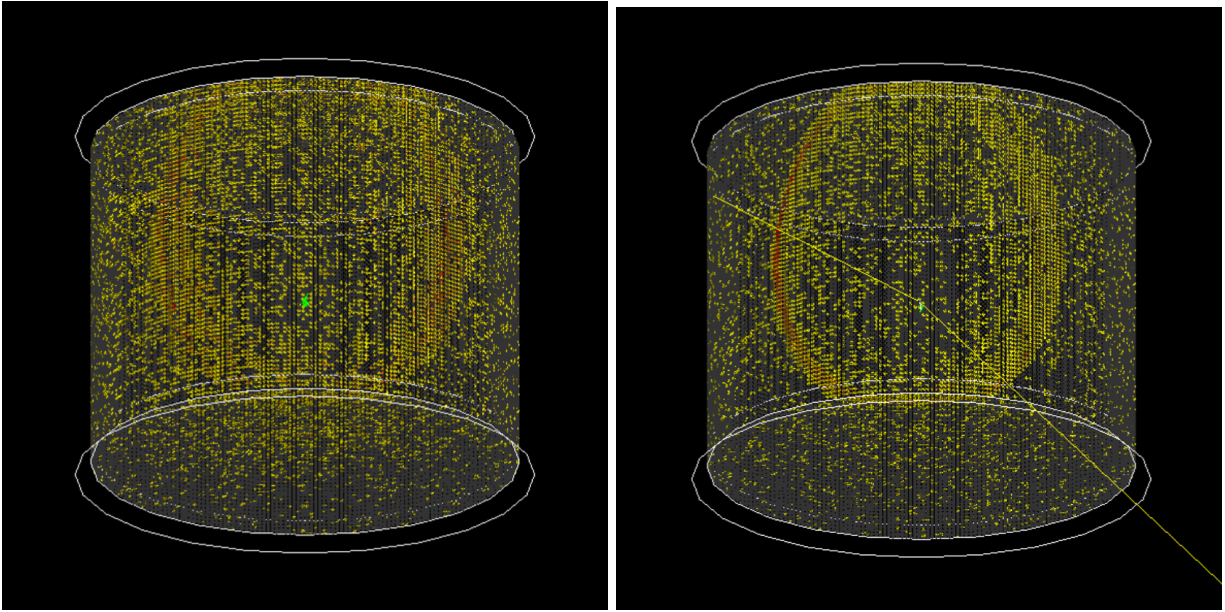


Figure 1: Simulated Cherenkov light detected from a 1 GeV electron (left) and muon (right) propagating in the Hyper-K far detector and detected by the ID PMTs.

218 neutral pion events, a critical background that could lead to the misidentification of these events as ν_e or $\bar{\nu}_e$.

219 Hyper-K will use the upgraded neutrino beam facility at J-PARC, currently serving T2K, and the ND
 220 complex at 280 m ¹ from the beam target, which includes the magnetised ND (ND280), the neutrino beam
 221 monitor (INGRID) and the water-based WAGASCI detector system, ready in day 1. Moreover, an Interme-
 222 diate Water Cherenkov Detector (IWCD), positioned at about 900 m from the neutrino production target
 223 will be built. It will span the neutrino beam at different off-axis angles using the “PRISM” technique [21].

224 The Water Cherenkov Test Experiment (WCTE) has been approved by the CERN SPSC and will take
 225 place in 2024 [22] with a prototype that will adopt the same water Cherenkov detection technology as IWCD.
 226 With a large overlap with the Hyper-K collaboration, its goal is to provide a platform to develop the percent
 227 level calibration techniques with particle fluxes of known type and kinematic properties as well as to probe
 228 important physics processes for the understanding of final state signatures, such as the production of high
 229 energy delta rays that produce Cherenkov light, the scattering and absorption of pions in the detector, and
 230 the secondary production of neutrons in the detector.

231 As shown in Fig. 2, the Hyper-K experiment will be able to achieve an unprecedented sensitivity to CPV.
 232 Both the high-intensity beam and the massive FD will allow to drastically increase the number of neutrino
 233 interactions compared to T2K and **precisely measure the CP violating phase (δ_{CP}) and will be able**
 234 **to exclude the hypothesis of CP conservation ($\sin \delta_{CP} = 0$)** for $\sim 60\%$ of possible true values of δ_{CP}
 235 at five standard deviations and $\sim 80\%$ at three standard deviations after 5 years of data taking. **After less**
 236 **than three years of data taking it will be possible to discover CPV if $\delta_{CP} = -\pi/2$.** Instead, in

¹The details of the handover of the ND complex at 280m from T2K to Hyper-K are currently under discussion.

237 the case of $\delta_{CP} = -\pi/4$, such discovery will be achieved with three more years of data, as shown in Fig. 3.
 238 Overall, δ_{CP} will be measured with a resolution better than 23° for any possible true value.

239 It is worth noting that, mostly thanks to the increased detection rate of the atmospheric neutrinos, also
 240 the MO can be determined with a significance between four and six standard deviations (depending on the
 241 true value of $\sin^2 \theta_{23}$) by combining neutrino accelerator and atmospheric data, as shown in Fig. 3. After six
 242 years of data taking a significance of four standard deviations could be already achieved. Moreover, Hyper-K
 243 will improve the resolution of the atmospheric parameters, $\sin^2 \theta_{23}$ and $|\Delta m_{32}^2|$, of the neutrino oscillation
 244 probability, respectively with a resolution as good as 0.015, depending on the actual value of the angle, and
 245 $1 \times 10^{-5} \text{ eV}^2$.

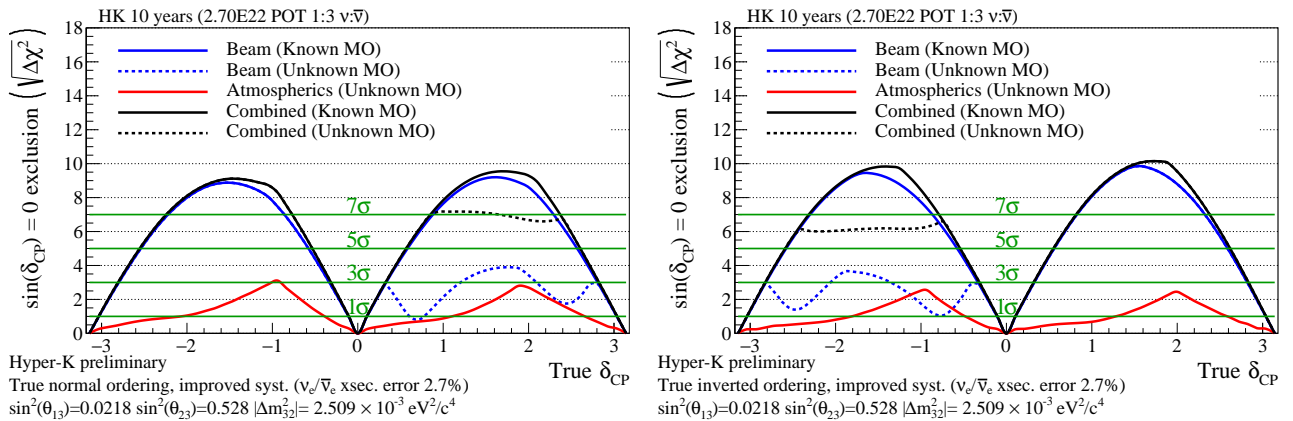


Figure 2: Left: Hyper-K sensitivity to exclude CP conservation as a function of the true value of δ_{CP} for 10 years data taking and true normal (left) and inverted (right) MO. The sensitivity is shown for neutrino accelerator (blue), atmospheric (red) and combined (black) data with both a known (solid line) and unknown (dashed line) MO. In case of unknown MO, the atmospheric sample allows to resolve the degeneracy between δ_{CP} and MO and achieve the 5 standard deviation sensitivity for the full range of δ_{CP} .

246 Hyper-K has a rich physics program beside its long baseline measurements [18]. Proton decay is a major
 247 physics target at Hyper-K, with the projected sensitivities surpassing limits from Super-K by approximately
 248 one order of magnitude for many decay modes. Hyper-K's increased fiducial mass and improved detection
 249 capabilities (as discussed above) will enable it to reach these limits both by accumulating larger exposures
 250 while suppressing atmospheric neutrino backgrounds.

251 If the proton decays into a positron and a neutral pion, as predicted by many GUT models, this process
 252 will be observed with more than 3σ significance if the proton lifetime is 10^{35} years or less. For GUTs
 253 incorporating SUSY, the favored decay into a neutrino and a positive kaon can be observed at the same level
 254 if the proton lifetime is 3×10^{34} years for the decay mode to a neutrino and a Kaon. It should be noted that
 255 various models predict many other possible decay modes. Hyper-K will have unprecedented sensitivity to
 256 these as well, enabling the discovery of multiple decay channels and possible determination of the underlying
 257 GUT symmetry.

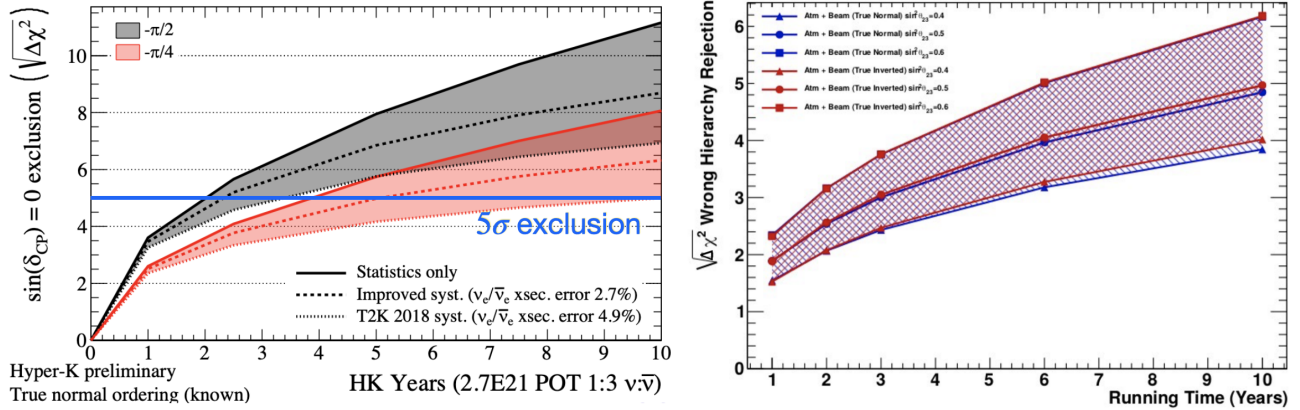


Figure 3: Left: Hyper-K sensitivity to exclude CP conservation for the case of true normal ordering as a function of running time assuming two different true values of $\delta_{CP} = -\pi/2, -\pi/4$ and different systematic uncertainty scenarios (T2K uncertainty in 2018, improved, only statistical) given known MO. Right: Hyper-K sensitivity to MO as a function of running time for different true values of $\sin^2\theta_{23}$ and for the case of both true normal (blue) and inverted (red) ordering [23]. It is obtained by combining accelerator and atmospheric neutrino data.

258 Further, Hyper-K has the potential to achieve new discoveries with observations of astrophysical neutrinos, such as solar and supernova neutrinos, and will play an important role in multi-messenger astronomy at 259 lower energies relative to the IceCube experiment. For example, Hyper-K’s measurement of solar neutrino 260 oscillations will probe matter effects in the Sun, confirming the upturn in the electron neutrino survival 261 probability at a few MeV predicted by the standard PMNS oscillation scenario or identifying a spectral 262 distortion consistent with exotic scenarios such as non-standard interactions. Due to its size, Hyper-K will 263 have unprecedented sensitivity to a galactic supernova neutrino burst and expects to record about 75,000 264 inverse beta decay events and 3,500 neutrino-electron elastic scattering events for a core-collapse supernova 265 at a distance of 10 kpc. With such high statistics the time variation of the neutrino event rate and energy 266 spectrum can be determined precisely, allowing for powerful model discrimination [24]. Similarly, the elastic 267 scattering measurement will allow Hyper-K to measure the direction to the supernova with an accuracy close 268 to one degree. Observation of the as-yet unmeasured diffuse supernova neutrino background (supernova 269 relic neutrinos) at more than 4σ is also expected. As the flux of this diffuse supernova neutrino background 270 depends on the frequency of supernova bursts in the early universe, Hyper-K’s observation will provide valu- 271 able information to constrain related processes and their corresponding models. Finally, Hyper-K’s size and 272 detection sensitivity will enable it to study other astrophysical neutrinos, dark matter annihilation in the 273 sun, Earth, and galactic center, as well as to search for other types of exotic particles.

274

275
 276 **The ambitious physics program of Hyper-K is supported by a well-defined roadmap and**
 277 **the realistic scenario for a potential discovery of leptonic CP violation within the next years.**
 278 The Hyper-K experiment will start collecting physics data in JFY 2027. The overall project schedule is

279 shown in Fig. 4. The cavern excavation has started and the access tunnel has been completed
 280 in February 2022. The excavation of the dome has also started and its diameter has already
 281 exceeded the Super-K one, as shown in Fig. 5. It will be completed by JFY 2024, when the tank
 282 construction and, later, the detector installation will start. In parallel, the PMT production has started
 283 and their installation will be completed by JFY 2026, together with the related electronics and mechanical
 284 equipment. The water filling step and the detector commissioning will take place over JFY 2026, before the
 285 start of the operation. The Hyper-K experiment will start collecting data for physics oscillation
 286 measurements in JFY 2027 with the full configuration, i.e. both the ND and the FD fully
 287 operative, with the potential of CPV discovery a few years after the start of data taking. As
 288 of 2023, the Hyper-K collaboration includes 21 countries, 101 institutes and about 560 people from all around
 289 the world.

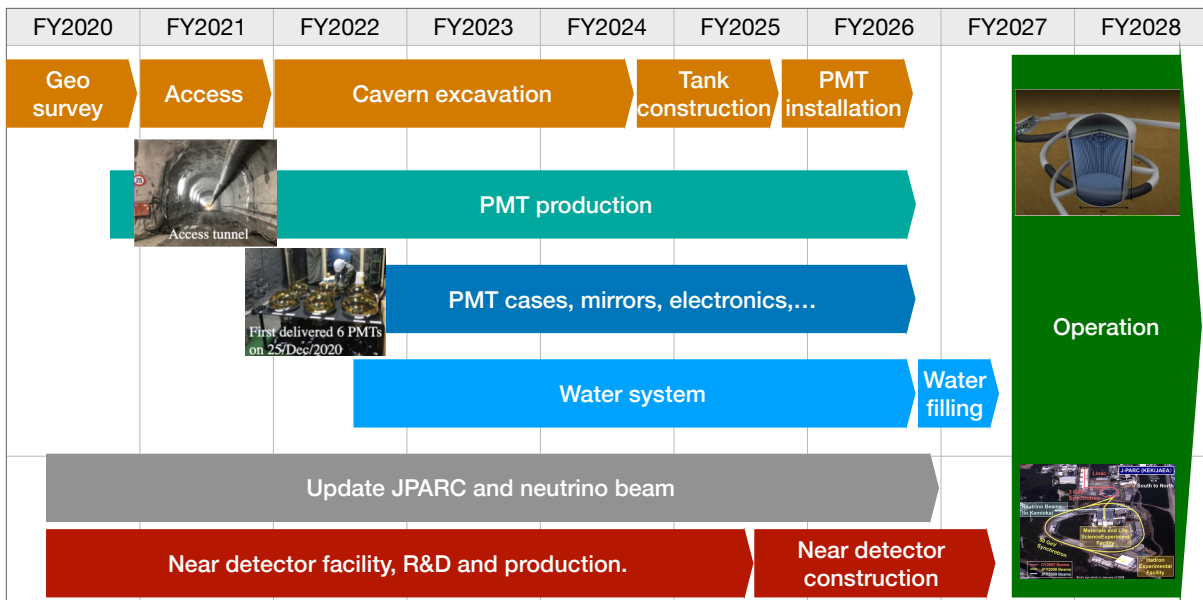


Figure 4: Hyper-K overall schedule in JFY towards the operation in 2027 [25].

290 3 The PMTs and the underwater electronics units

291 The integration of the PMTs inside the Hyper-K FD is shown in Fig. 6. The PMTs will detect the Cherenkov
 292 light produced by the charged particles propagating in the ultra-pure water inside the tank. The PMTs will
 293 be fixed to a mechanical frame and will surround the full water volume.

294 Three types of PMTs, which differ in size and granularity, will be used in Hyper-K: 20-inch Hamamatsu
 295 PMTs for the ID, 3-inch Hamamatsu PMTs for the multi-PMTs (mPMTs) of the ID, and 3-inch Hamamatsu
 296 or NNVT PMTs, but both satisfying the same criteria, for the OD. The 20-inch and the 3-inch PMTs are
 297 shown in Fig. 7 while the characteristics of both PMTs are shown in Tab. 1. For simplicity only the 3-inch



Figure 5: The status of the cavern excavation as of June 2023 is shown, the access tunnel (left) and top part of the dome (right) that will host the Hyper-K water tank.

298 Hamamatsu PMT for the OD is shown. Compared to the Super-K one, the Hyper-K 20-inch PMTs will
 299 profit of a better timing resolution for vertex reconstruction (1.5 ns), a charge resolution (30.8%), and a
 300 photodetection efficiency (PDE) all higher by a factor two. About 20,000 20-inch PMTs will provide a
 301 photocoverage of the ID of about 20%, lower by a factor two compared to Super-K, whilst maintaining an
 302 overall better performance. 3,600 3-inch PMTs will be used for the OD. In order to enhance the overall
 303 light yield, they will be mounted on wavelength shifting plates that, thanks to high-reflectivity Tyvek, will
 304 maximize the amount of light at the PMTs.

	Hamamatsu R12860-HQE	Hamamatsu R14374
Photocathode diameter	20 inches	3 inches
Sensitive wavelength range	300–650 nm	300–650 nm
Peak sensitive wavelength	420 nm	420 nm
Gain	10^7 at $\sim 2000V$	5×10^6
Dark pulse rate	6 kHz at 10^7 gain	< 1.5 kHz
Operational temperature	5–35 °C	-10 to 50 °C
HV resistance	5.9 M Ω	10.7 M Ω
HV range	0-2600 V	0-1500 V

Table 1: Characteristics of the Hyper-K PMTs.

305 The multi-PMTs are a particular configuration that replaces a single big PMT with different smaller ones.
 306 These multi-PMTs show different features in the output charge signal, hence the design and configuration of
 307 the readout electronics and related components are quite different from those of 20-inch and 3-inch PMTs.
 308 As a consequence, the multi-PMT electronics system uses a different scheme for the signal digitization and

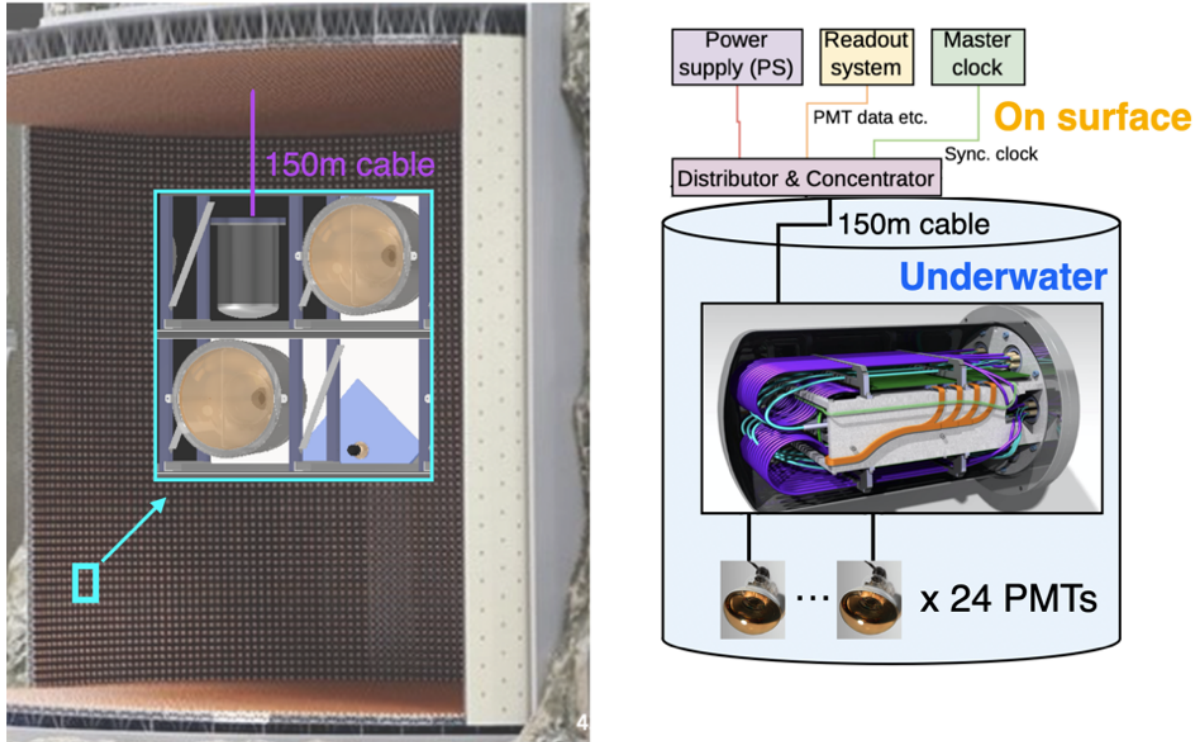


Figure 6: Left: inner view of the Hyper-K ID. A zoomed view on two 20-inch PMTs installed on the mechanical frame together with an underwater unit is shown. Right: CAD design of the underwater electronics unit and block diagram of the FD electronics from PMTs to the DAQ system.

309 the data transfer to the DAQ system, thus it does not use the electronics units to be assembled at CERN.
 310 The mPMTs assembly is not part of this LoI and it will be realized in dedicated infrastructures set up by
 311 the institutes involved in the mPMTs project.

312

313 Overall, around 900 underwater electronics units (including spares) will operate the ID and OD PMTs.
 314 There will be two variants of these units, one handling only the 20-inch PMTs (so called “pure-ID” type) and
 315 the other handling both 20-inch PMTs and 3-inch PMTs (the “hybrid ID+OD” type).

316 In the pure-ID type, twenty-four different 20-inch PMTs are connected via ~ 20 meter long cables to
 317 the corresponding electronics unit, also placed underwater. A single underwater electronics unit provides
 318 high voltage to the PMT bases, independently digitizes the analogue signal of each PMT and sends it to the
 319 out-of-water Data Acquisition System via optical cables of lengths up to ~ 150 meters. This configuration
 320 will allow to have a short distance between the front-end electronics and PMTs. The main advantages are
 321 the lower signal attenuation and suppression of electromagnetic interference pickup. Moreover, thanks to
 322 reduced cable length (thus lower weight), the PMT and electronics support structure would be simpler, thus
 323 allowing for cost savings. On the other hand, this implies that the front-end electronics, Low Voltage (LV)
 324 and High Voltage (HV) power supplies will not be accessible during the filling of the detector tank, which

325 takes about 6 months, as well as during the operation, once the FD tank will be filled with water. Hence,
326 long-term reliability of these components is essential for collecting high-quality data. The requirement is
327 that the number of dead acquisition channels after ten years of detector running will not exceed the 10% of
328 the total number of channels. Since the unit is underwater and exposed to high pressure, all the components
329 will be placed inside a stainless steel water-tight vessel. In total, about 560 pure-ID underwater electronics
330 units will operate the 20-inch PMTs of the ID.

331 The hybrid ID+OD unit is very similar to the pure-ID one described above but will operate twenty
332 20-inch PMTs as well as twelve 3-inch PMTs. A few additional circuit boards as well as small differences
333 in the design related to the PMT signal digitizer board and their integration in the mechanical vessel are
334 needed. More details can be found respectively in Sec. 3.1.1 and Sec. 3.1.6. In total about 320 hybrid units
335 will operate a fraction of the ID 20-inch PMTs and all the OD 3-inch PMTs.

336 **This Letter of Intent proposes to assemble at CERN the underwater electronics units that**
337 **belong to the 20-inch ID and 3-inch OD PMTs.**

338

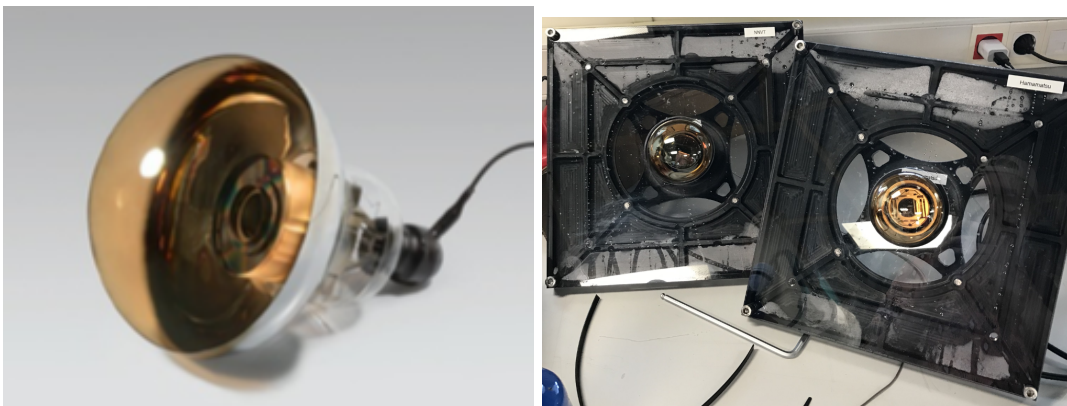


Figure 7: Left: 20-inch PMT of the ID. Right: 3-inch PMT of the OD right after tests in water.

339 3.1 The electronics underwater unit

340 The underwater electronics unit contains those components that stay underwater near the PMTs to provide
341 them the High Voltage (HV), the Low Voltage (LV), and digitize their signals to provide time and charge
342 estimates, that are subsequently transmitted to the on-surface data acquisition system via $O(100\text{ m})$ optical
343 cable.

344 The CAD design of an underwater unit is shown in Fig. 6. Its block diagram is shown in Fig. 8. It
345 comprises the two PMT signal digitizer boards, the HV power supply, the LV power supply and regulator,
346 the slow monitor and control, the synchronization system. All the components are embedded inside a stainless
347 steel water-tight vessel. Each vessel serves twenty-four 20-inch PMTs or twenty 20-inch PMTs plus twelve
348 3-inch PMTs. The PMT cables enter the underwater unit through six feedthroughs (PMT FTs). Each

349 feedthrough for 20-inch PMT hosts four PMT cables, each of which conceals two coaxial cables, one for
 350 signal and the other for HV. The feedthrough for 3-inch PMT hosts 12 coaxial cables, each of which carries
 351 both HV and signal.

352 A central “communication” feedthrough (COM FT) hosts two copper cables with a length up to about
 353 150 m that brings from on-surface the +48 V / ~2A power and return to the LV power supply board inside
 354 the vessel, which then provides power to the other underwater components, and twelve optical fibers to send
 355 the PMT digitized signals to the on-surface DAQ system and the reference clock along with intertwined data
 356 transmission for timing-sensitive (deterministic) control signals.

357 Three 12 V outputs with various currents (from 1 to 2 A) are provided to the two digitizers and one data
 358 processing board (DPB). A 48 V output is sent to the 24-channel HV power supply board. Then the HV is
 359 supplied to the 24 ID PMTs, up to 2.6 kV voltage output at 0.5 mA with voltage setting resolution < 0.2%.
 360 The same HV board is used to feed the OD PMTs, which operate in the range of 900 V to 1500 V.

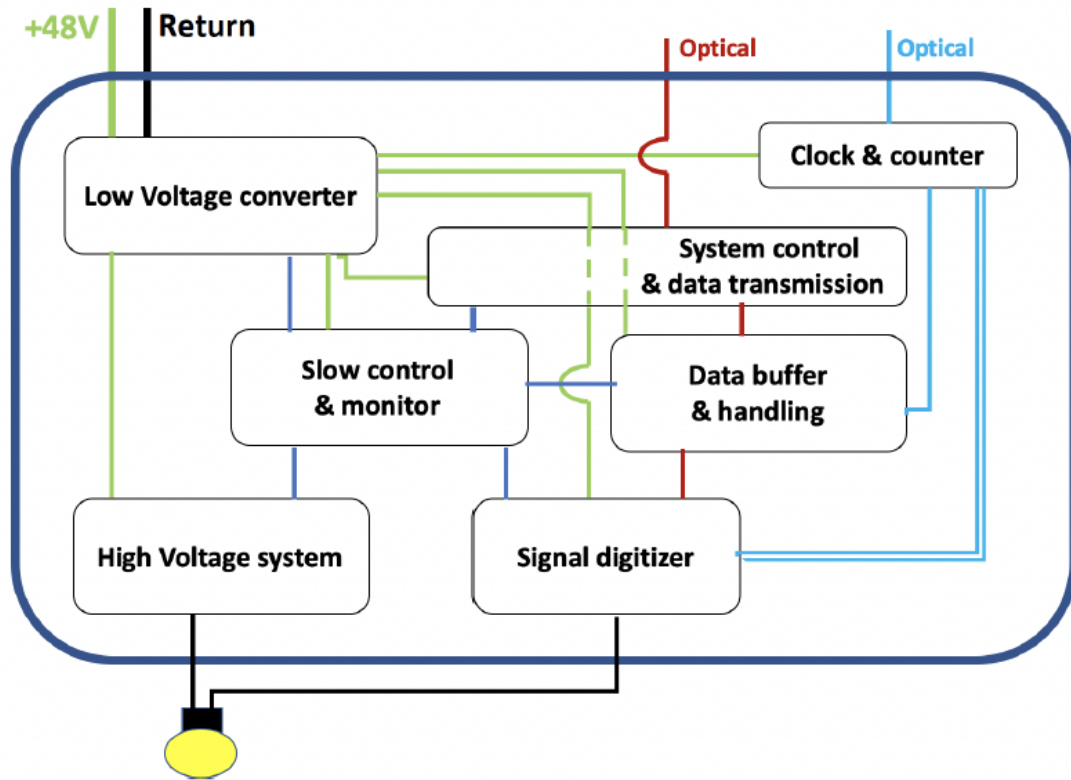


Figure 8: Block diagram of the underwater unit electronics.

361 **This LoI is focused on the test and the assembly of the underwater units for the ID and**
 362 **OD parts of the FD.** In the next sections a more detailed description of each unit sub-system component
 363 is given.

364 3.1.1 The digitizer

365 The signal digitizer block accepts PMT analog input signals and outputs the digitized timing and charge
 366 values. This implies that each channel of the digitizer must be equipped with a discriminator or has an
 367 equivalent mechanism. In order to have a sufficiently high efficiency to record 1 photoelectron (pe) level
 368 signal, the threshold level is required to be set at $\sim 1/6$ pe. Since the expected number of pe could exceed
 369 1,000, the electronics is required to have at least a dynamic range up to 1,250 pe and a linearity of the
 370 measured charge better than 1% from 1 pe to 1,250 pe. Furthermore, the charge resolution is required to
 371 be better than 0.5 pe (RMS) for signals below 25 pe. Accuracy of the timing is critical in reconstructing
 372 the vertex. The least significant bit (LSB) of the timing is required to be smaller than 0.5 ns and to have
 373 a resolution better than 0.3 ns for 1 pe and 0.2 ns above 5 pe. All the channels have to be synchronized and
 374 the relative difference has to be stable within 0.1 ns.

375 The basic idea is the implementation of the analog front-end using discrete integrated circuits (IC). The
 376 block diagram of the circuit of a single digitization channel is shown in Fig. 9. The circuit is divided into
 377 3 sections: the *input receiver*, the *timing* path implemented by a fast discriminator which provides a fast
 378 signal that marks the beginning of the hit, and the *integration* path, which converts the charge of the hit to
 379 a voltage level, that is then sampled by an ADC.

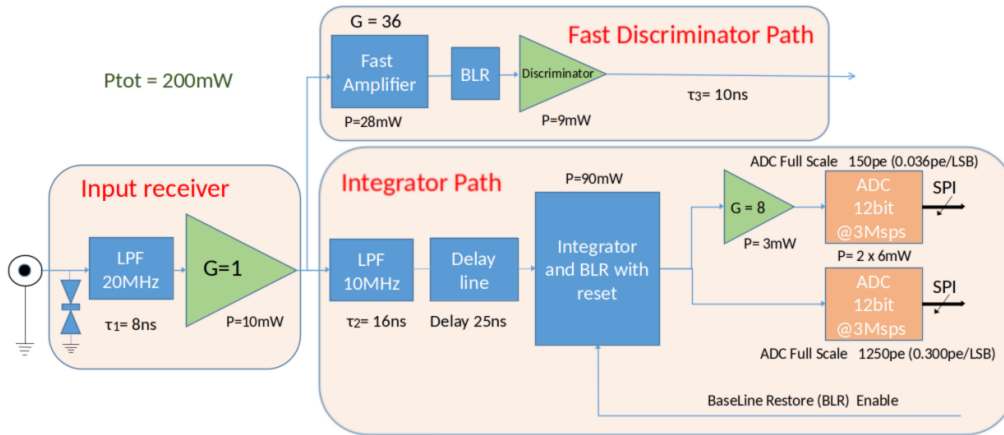


Figure 9: Front End circuit block diagram. The three main blocks are highlighted: the input receiver, the timing path, and the integration path.

380 The input signal is AC coupled to the circuit by a capacitor which allows to adapt the baseline to the
 381 requirements of the power supply of the circuit. A buffer is used to achieve wideband impedance matching
 382 and to feed both the fast discriminator path and the integrator path without affecting the input signal itself.
 383 To protect the input circuit from Electro-Static-Discharges (ESD) and over-voltages, there are 4 precautions:
 384 firstly, there is a *Gas Discharge Tube* to protect the receiver from HV spark coming from the PMT; then
 385 there is a *Transient Voltage Suppressor* (TVS) and a clamping diode. Last, but not least, the 100 Ohm series

386 resistors help limiting the input current fed to the clamping diode and the TVS.

387 The discriminator path consists of an amplifier with such a high gain ($G \sim 36$) that the amplifier itself
388 is promptly saturated and its response is fast and repetitive. Such amplification is obtained with a BJT
389 transistor followed by an operational amplifier. The threshold can be set by a suitable DAC not shown in the
390 block diagram. A traditional baseline restorer circuit prevents baseline shifts resulting from AC coupling,
391 PMT pulse overshoots and signal rate variations. A time walk effect is observed in the discriminator output,
392 especially for low amplitude signals, with an approximate inverse dependence on hit amplitude. Such effect
393 will be minimized using the information of the measured charge, after a careful calibration of the circuit.

394 The integrator is the other fundamental block in the acquisition chain, since the charge resolution depends
395 on it. To stabilize the integrator baseline value, a feedback system will constraint the voltage value on the
396 input of the circuit at a predetermined value, that in our case was set at 200 mV. During the integration phase,
397 which is triggered by the discriminator in the timing path, the feedback loop is opened by the *BLR_Enable*
398 logic signal shown in Fig. 9. The *BLR_Enable* signal, which enables the integration of the input signal, is
399 generated by the FPGA using combinatorial logic, in order to reduce as much as possible the time to open
400 the BLR feedback loop. To compensate this delay, which sums up to ~ 15 ns, a delay line of 25 ns is included
401 in the integrator block.

402 After a programmable amount of time, the FPGA generates the *convert* signal for the ADC to freeze the
403 integrated value and start the acquisition. After issuing the conversion signal, the FPGA logic can reset the
404 integrator, closing again the feedback loop on the Baseline Restore circuit.

405 Due to the huge dynamic range and the very high resolution required on the charge digitization, two gain
406 paths with two ADCs are used. The gain ratio of the two signal paths is about 8; for each event signals from
407 both low- and high-gain paths are acquired and stored; later on it is possible to choose in the FPGA logic
408 the most suitable value between the two. Each ADC has a maximum sampling frequency of 3 MHz and a
409 resolution of 12 bit, with a power dissipation of 6.5 mW.

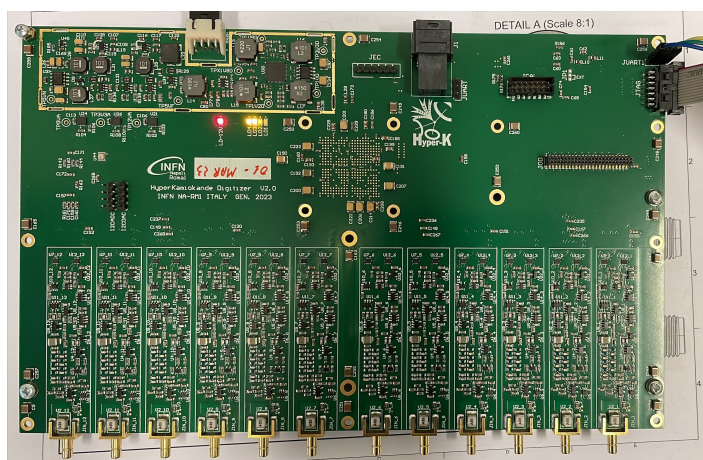


Figure 10: Picture of ID digitizer first prototype board.

410 The digitizer board is shown in Fig. 10: there are the 12 input channels to take data from PMTs, the
411 power section, the FPGA to drive all the logic signals, the *MiniSAS* connector to exchange data and control
412 signals with the DPB board (see 3.1.2 paragraph). The board features a bunch of sensors to monitor the
413 state of the board itself and also of the environment (temperature, and pressure, just to name a few); there
414 is a calibration circuit to check performance consistency, and a connector dedicated to OD board connection.

415
416 As described above, there will be a mixture of electronics underwater pure ID units and hybrid ID+OD
417 units. For the latter, there is a dedicated OD PMT digitizer and HV splitter board to process the OD signals.
418 This board digitizes the OD PMT signal and sends the digital data to the ID digitizer board. One important
419 difference between the OD PMTs and the ID PMTs is that there will be a single cable attached to the OD
420 PMTs (compared to one HV and one signal cable attached to the ID PMTs). This design choice was carried
421 out to simplify the OD design and to reduce cost. This necessitates the use of a HV splitter input stage to
422 the OD boards to ensure that the high voltage and the PMT signal are decoupled in the board. Otherwise,
423 the signals are processed in a very similar way, with an input receiver stage, fast amplifier and discriminator
424 path, and an integrator path connected to the ADC. The design of the ID and OD circuits is very similar,
425 but the OD design can be further simplified due to the relaxed requirements of the OD boards. The input
426 receiver has an input bandwidth of 80 MHz (due to the faster 3-inch signals), and only one gain (as opposed
427 to two gains) before the ADC, due to the reduced dynamic range requirement of the OD PMTs (from 0.25 pe
428 to 100 pe).

429 The design of the OD board is at an advanced stage, nearly ready for prototyping. A schematic of the
430 6-channel OD board can be found in Fig. 11. The HV splitter portion of the OD board is seen on the bottom
431 part of the OD splitter/digitizer board. The board will have two HV connectors and six connectors to the
432 PMT. A single HV channel powers three PMT channels. The six individual digitizer channels can be seen
433 on the upper part of the board. A 50-pin connector will connect to the main digitizer board that will drive
434 its operation.

435 3.1.2 The Data Processing Board

436 The Data Processing Block (DPB) implements three functionalities in the front-end electronics block diagram
437 (Fig. 8):

- 438 • data processing and network interface (data buffer and handling, system control and data transmission),
439 which requires a large buffer to handle supernova events, preventing network congestion in the DAQ, a
440 processor running Linux to implement ZMQ protocol for the DAQ and redundant optical transceivers
441 for DAQ;
- 442 • synchronization (clock + counter), which requires a clock synthesizer and feedback loop as well as

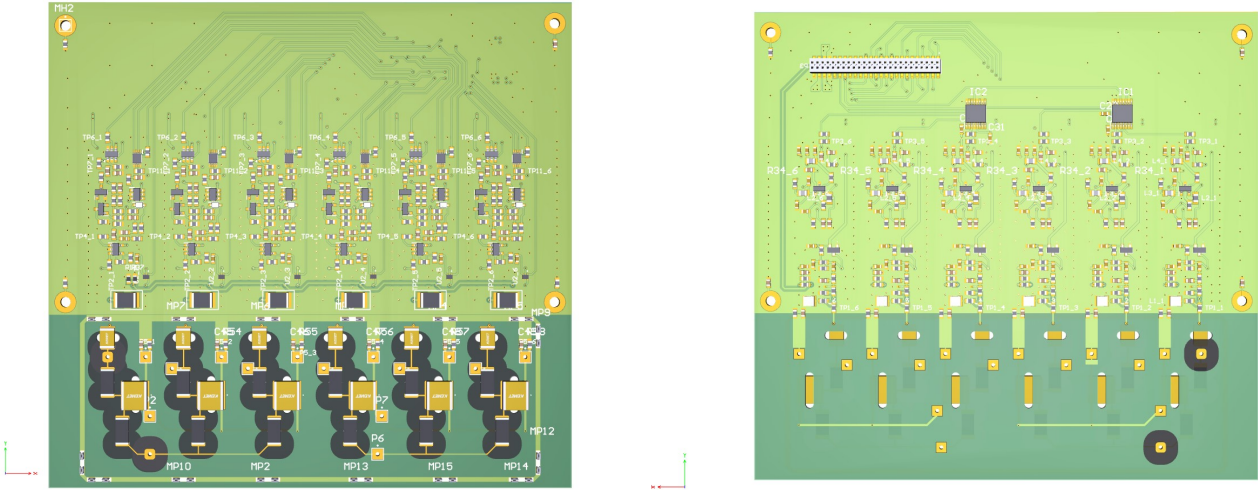


Figure 11: Schematic of OD Digitizer. Top view (left) and bottom view (right).

443 fanout to send copies to other units; redundant optical transceivers for the timing & sync system;
 444 • slow control and monitor, which requires RS-485 interfaces for HV and LV modules, serial port and
 445 JTAG to interface digitizers.

446 The requirements listed above have been met in the DPB prototype with a combination of a SoM (System-
 447 on-Module) and a baseboard that adds communication interfaces and other features missing in the SoM.
 448 The SoM is a Mercury+ XU8 from Enclustra company. The SoM includes a Xilinx Zynq Ultrascale+ with
 449 dual ARM Cortex-A53 running Linux, ECC DDR4 memory, QSPI and eMMC boot memories (Fig. 12), as
 450 well as a number of high-speed serial interfaces.

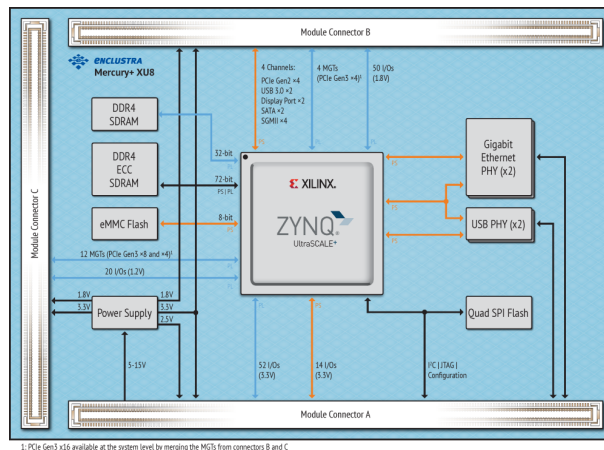


Figure 12: Block diagram of the SoM module for the DPB.

451 The DPB2 prototype will equip a ME-XU8-4CG-1E-D11E-R2.2 SoM with 4 GB ECC DDR4 memory,
 452 though 8 GB are intended for the final production units. The module equips a XCZU4CG-1FBVB900E
 453 Zynq Ultrascale+ SoC. The baseboard has been jointly designed with Enclustra, in order to reduce risks

454 and speed-up development. Fig. 13 shows the top and bottom board views, indicating the main I/O and
 455 components.

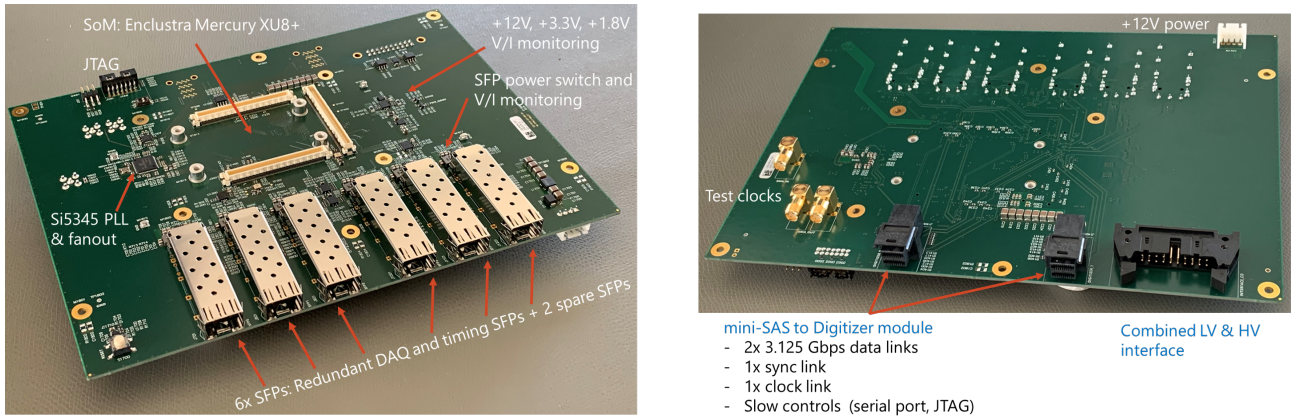


Figure 13: DPB hardware overview: top (left) and bottom (right) side.

456 3.1.3 The Low Voltage modules

457 Each underwater vessel will serve twenty-four ID PMTs through six PMT FTs. Each FT hosts four HV
 458 cables (modified RG-174/U cable) and four signal cables (RG-58). An external power supply is located out
 459 of the water tank and connected to the underwater unit through COM FT via two copper cables with lengths
 460 up to about 150 m each in the range of +40 to +55 V. It will provide ~ 2 A of power and “Return” for the
 461 electronics through a low voltage power supply board inside the vessel. The long cable can pick up voltage
 462 and current noise from various disturbances, such as electrostatic discharges, high frequency electrical fast
 463 transients, surge transients, over-voltage, etc. In order to avoid any damage to the front-end electronics,
 464 protection circuits, and noise filters are implemented.

465 As seen in Figure 14, the LV board includes redundant isolated DC-DC converter, providing isolation
 466 between the input and the output and referenced to its local ground on the LV board. The local ground is
 467 then connected to the output section with optional mounting points allowing its connections to the vessel
 468 ground.

469 Since the LV board will have to function for years without being replaced, its long-term reliability is
 470 essential. For this reason, redundant components are included for the critical elements, such as the DC-DC
 471 converter, the micro-controller, the step-down as well as the environmental sensors as depicted in the LV
 472 block diagram.

473 The LV boards provide three 12 V outputs with various currents, up to 2 A, for two digitizers and one
 474 data processing board. As shown in Fig. 14, one of the 48 V power line voltages coming out of the EMI
 475 filter and 48V-to-48V DC-DC converter is used as an input for the HV board, i.e. 48 V with current around
 476 1.5 A. Such configuration will allow to improve the reliability of the whole system. Tab. 2 summarizes the

477 power requirements on the LV board. Since the LV power supply board is placed underwater inside the
 478 watertight vessel and provides the power to the rest of the electronic payload, its overall reliability must be
 479 ensured, and its failure rate must be kept below 1% per board for 10 years of operation. We consider the
 480 board failed if any of the following conditions are met: failure of the input filter; complete failure of the
 481 redundant isolated DC-DC converter; complete failure of redundant CPU; complete failure of slow control
 482 link; complete failure of the 12 V output to the data processing board. In case of a failure of the 12 V output
 483 to one of the digitizers, we assume half of the board is malfunctioning.

484 The LV board will be remotely controlled and monitored using the RS485 communication interface. It
 485 allows switching ON/OFF each channel independently and remotely, except the always-ON auxiliary output
 486 channel used by the data processing board. In addition, with existing environmental sensors on the board,
 487 it will provide information on the temperature, humidity, pressure, and water leak inside the vessel. The LV
 488 board also provides monitoring input voltage and currents for each channel. Last but not least, the power
 489 efficiency of the LV board must be higher than 84% above 60% of full load (100 W delivered at full load), in
 490 order to minimize the heat deposition in the vessel.

Unit Component	Supply Voltage	Power	Current
Input to Low Voltage module			
Low Voltage	+48 V	100 W	< 2.5 A
Input to electronics components from Low Voltage module			
High Voltage	+48 V	~ 45 W	1.5 A
Digitizer board #1	+12 V	~ 7.5 W	< 1 A
Digitizer board #2	+12 V	~ 7.5 W	< 1 A
Data processing board	+12 V	~ 25 W	1.25 A

Table 2: Input to LV modules and corresponding outputs to the other underwater electronics components.

491 3.1.4 The High Voltage modules

492 In Hyper-K, PMTs will operate at around 900 V to 1500 V for the OD and 1400 V to 2600 V for the ID
 493 using precisely controlled high voltage power supplies and with very low ripple requirements. The maximum
 494 current is 500 μ A. It is important that the high voltage applied to the PMT is stable since it affects
 495 the stability of the PMT gain. A variation of the high voltage induces a gain variation, deteriorating the
 496 measurement of the energy deposited by particles.

497 The HV board will supply 24 voltage outputs via six 4-channel connectors compatible with RG-174/U
 498 cables, regulated between 20 V and 2600 V with a maximum current of 500 μ A and independently settable

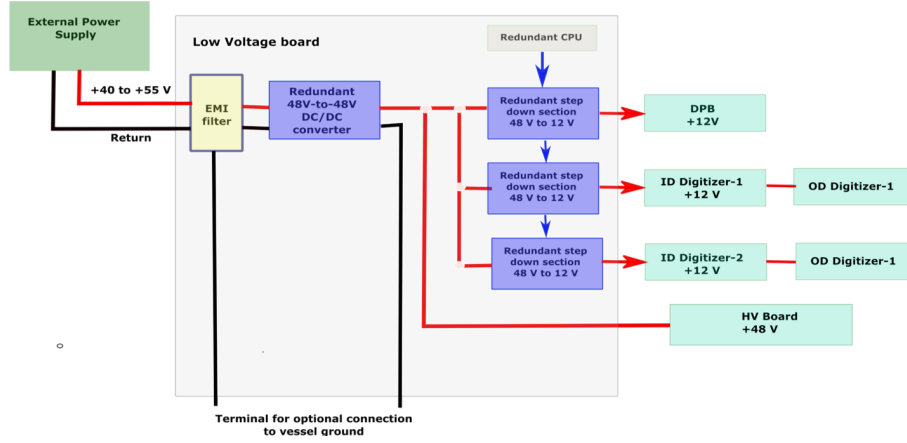


Figure 14: Low Voltage power supply board block diagram.

499 with a precision of $\pm 1\%$ in the range of 900 V to 2600 V. The applied high voltage must be stable, with
 500 a spread better than $\pm 0.2\%$ per year for long term operation, ensuring a ripple smaller than 100 mV peak
 501 to peak from 10 Hz to 10 kHz and 10 mV peak to peak from 10 kHz to 20 MHz. All output channels are
 502 software configurable ramp-up and ramp-down voltage rates from a minimum of 1 V/s to a maximum of 500
 503 V/s with a step of 10 V.

504 The HV board can be remotely controlled and monitored via RS485 communication interface, allowing
 505 to set, monitor and adjust each individual channel. To maximize the ability to operate of the detector in case
 506 of problems, the HV board allows to control individual channels; it is required that one or more channels
 507 can be operated normally while some other channels are inhibited, i.e. switched off. The precision of voltage
 508 and current monitoring is better than $\pm 1\%$ and $\pm 2\%$ respectively, in the range of 900 V to 2600 V. The
 509 HV board will be equipped with overvoltage, undervoltage and overcurrent protections. Occurrence of any
 510 of these fault conditions will cause the channel to be switched off. The status of each channel is monitored,
 511 including its temperature.

512 The electronics unit in Hyper-K will be placed inside a watertight vessel submerged in water, without
 513 access for about 10 years. Therefore, long-term reliability and redundancy are crucial also for HV boards.
 514 The average HV channel failure rate must be less than 1% for 10 years of operation. Fig. 15 shows the HV
 515 block diagram with possible redundant components.

516 The allowed power consumption and heat dissipation of the electronic units is limited by the cooling
 517 capability inside the underwater vessel. The heat dissipation on the HV board is limited to less than 24
 518 W. In other words, the board efficiency must be better than 50% at a voltage of 2500 V and a load of 5.9
 519 M Ω . The HV board must be hosted in a metallic case, behaving as EMI shield. To ensure the stability
 520 of the electrical performance and its reliability, and to have the temperature inside the pressure vessel stay
 521 within the maximum allowable temperature, the HV board must be designed in such a way that the heat
 522 dissipation is channeled through the “bottom” face of the metallic case. This face will be the “fixing side” of

523 the mechanical support inside the underwater vessel, which acts as a thermal contact for heat dissipation.

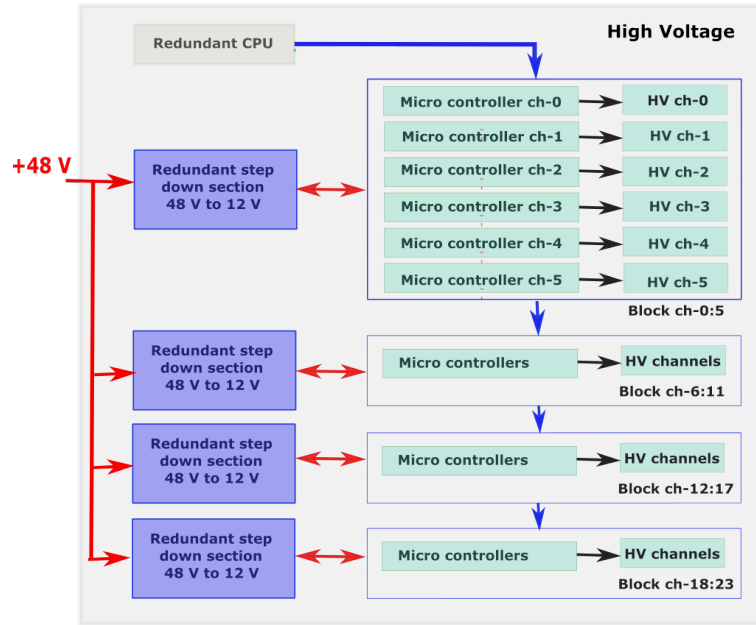


Figure 15: High Voltage power supply board block diagram.

524 3.1.5 The time synchronization

525 A crucial piece of information to reconstruct the Cherenkov ring(s) associated with an event in the Hyper-
 526 Kamiokande experiment is the arrival time of the light emitted in water on the detector's PMTs. To achieve
 527 this goal a reference time must be established and distributed to all the PMT front-end (FE) module readout
 528 electronics.

529 The time synchronization precision is directly related to the event's reconstruction accuracy; therefore,
 530 great care must be devoted to this task to control all sources of errors and inaccuracies. The Hyper-
 531 Kamiokande experiment requires a time distribution jitter smaller than 100 ps RMS and the clock skew
 532 between front-end boards to be constant over any power-on and reset.

533 The time tag of each particle interaction needs to be in a format that allows its correlation with data
 534 collected by other experiments worldwide; for this reason, the generated local time base has to be associated
 535 with the Coordinated Universal Time (UTC) with an accuracy better than 100 ns. This absolute time
 536 tagging will also be used to identify the events generated in the detector by the particles sent from the
 537 J-PARC accelerator. Along with the time synchronization, some "critical information" like slow control data
 538 have to be transmitted by this subsystem hence a 100 Mbps or greater bandwidth bidirectional data channel
 539 must be provided.

540 The full block scheme of the proposed system is depicted in Fig. 16.

541 To guarantee the most stable and precise reference, the local time base originates in an atomic clock

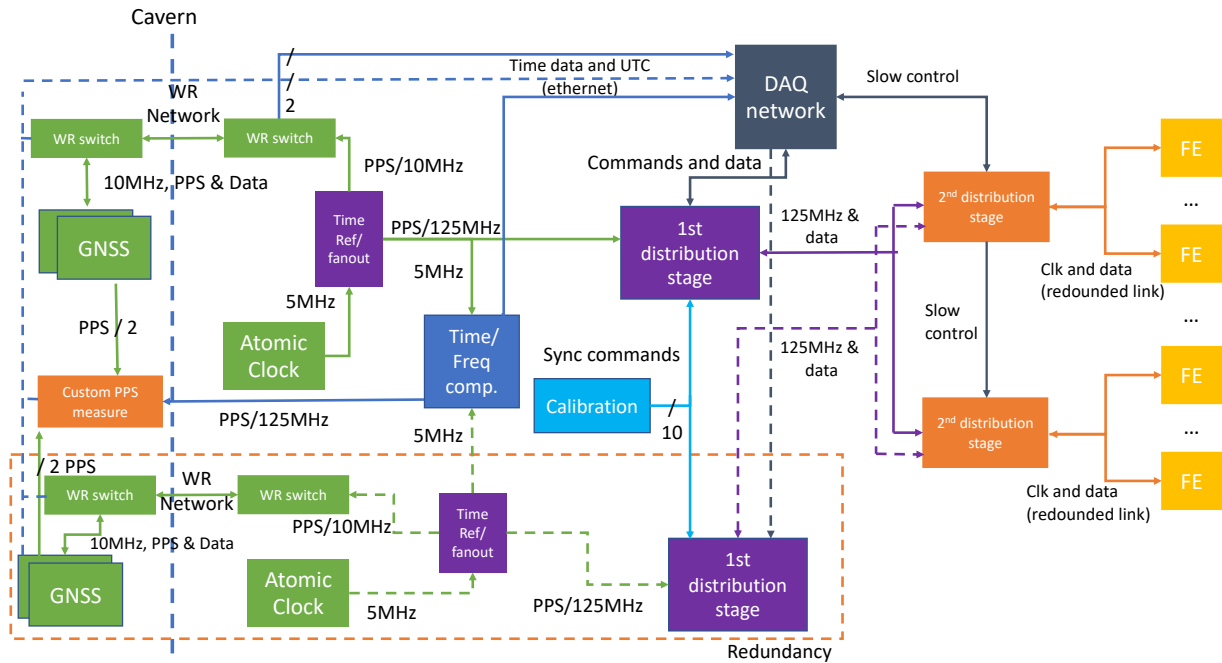


Figure 16: The proposed time distribution block scheme. The green boxes are part of the clock generation and UTC tagging. The purple elements constitute the first distribution stage, the orange ones are for the second distribution stage, while the yellow ones refer to the time distribution endpoint, part of the front-end.

542 working in free-running mode. It generates a 5 MHz frequency that is sent to a time reference fan-out
 543 board. Here the 125 MHz reference clock is generated and sent to the distribution network along with a
 544 PPS (Pulse Per Second) "counted" using the 5 MHz time base. The 125 MHz frequency is distributed over
 545 different branches by means of time distribution modules and delivered to all the leaves represented by the
 546 FE modules using the so-called Time Distribution Endpoints or TDE embedded on the DPB. A 10 MHz
 547 clock is also generated and sent to a GNSS (Global Navigation Satellite System) along with the PPS. Here
 548 the time distance between the local PPS, the GNSS time and, in turn, a UTC prediction is measured and
 549 sent to the data acquisition computer infrastructure via Ethernet protocol where it is used to convert the
 550 event's local time tag to it. The PPS signals from the GNSS receivers will be also compared directly to the
 551 locally generated one using a custom board. This feature will be used to double check the performances of
 552 the satellites receivers.

553 3.1.6 The water-tight vessel

554 The water-tight vessels and the electronics stand are the mechanical parts where the different electronics
 555 components are assembled and hosted underwater in a safe environment. The importance of the vessels is
 556 that it must remain water tight under a pressure up to about 7 bars in ultra-pure water. Even if, initially, the
 557 Hyper-K FD will not contain Gadolinium (Gd), like currently Super-K does to enhance the neutron capture,

558 the collaboration decided to still keep the option of adding Gd doping in the future. For such reason, the
 559 design complies also with the case of Gd doped water. The material for the vessel is passivated Stainless Steel
 560 304, which has been used in Super-K and its compatibility with ultra-pure and Gd-loaded water is firmly
 561 established. The electronics stand is a relatively simple aluminum support fixed at the flange inside the
 562 vessel. Its purpose is to host the electronics components (two digitizer boards, DPB, HV and LV modules)
 563 and transfer the heat to the water outside the vessel. Each underwater vessel that will host the components
 564 for the ID-related PMTs will have six feedthroughs, which will include the high voltage and signal cables for
 565 four PMTs each, giving a total of twenty-four PMTs that will be supplied by each vessel. Each feedthrough
 566 hosts four composite cables and is composed of a 90 mm long polyethylene mold that is attached to each of
 567 the six pass-through holes of the cover flange using a silicon gasket. A very similar design is also adopted for
 568 the hybrid configuration, which will support 20 ID and 12 OD PMTs. The CAD model of the underwater
 569 vessels are shown in Fig. 17.

Nominal water pressure	7 bar
Pressure and tightness test	10 bar
Total heat cooling through flange or vessel	75 W
Max Total weight	60 kg
Envelope volume	400 mm × 400 mm × 550 mm

Table 3: Requirements on the water-tight vessel.

570 In Tab. 3 the requirements on the vessel design are listed. Pressure and tightness test was successfully
 571 performed at the Paul Scherrer Institute (PSI) and officially protocolled. The vessel stayed water tight for
 572 the entire test and absolutely no mechanical deformation was observed.

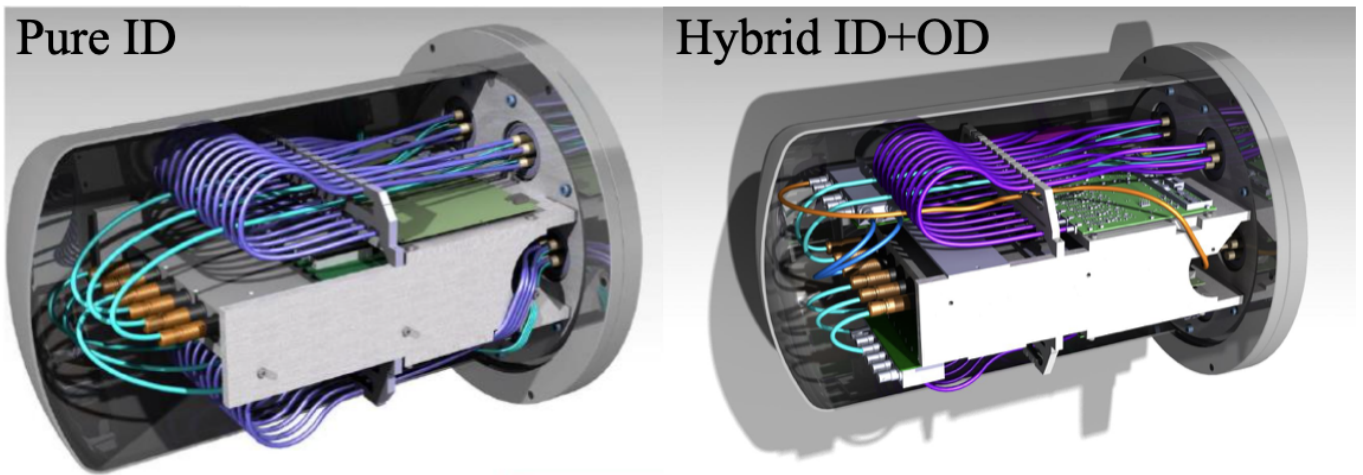


Figure 17: 3D model of the pure ID (left) and hybrid ID+OD (right) underwater vessels.

573 The total number of vessels and electronics stand is 560 for pure ID units and 320 for hybrid ID+OD
 574 units. The vessel final design is the result of many iterations and optimizations. A compromise was sought in
 575 the geometry in order to use parts available on the market and, consequently, minimize the overall production
 576 costs by avoiding, where possible, custom made parts. The exact same strategy applies for the design of
 577 the electronics stand whose choice of material, geometry and manufacturing process are the result of an
 578 optimisation path seeking the best balance between cost and design. Everything is also optimized from the
 579 point of view of the assembly by simplifying, where possible, the assembly procedure whilst always prioritizing
 580 the safety of the equipment inside the vessel. The 2D drawings of the designed vessel and electronics stand
 581 as well as the results of the Finite Element Analysis (FEA) studies are shown in Fig. 18.

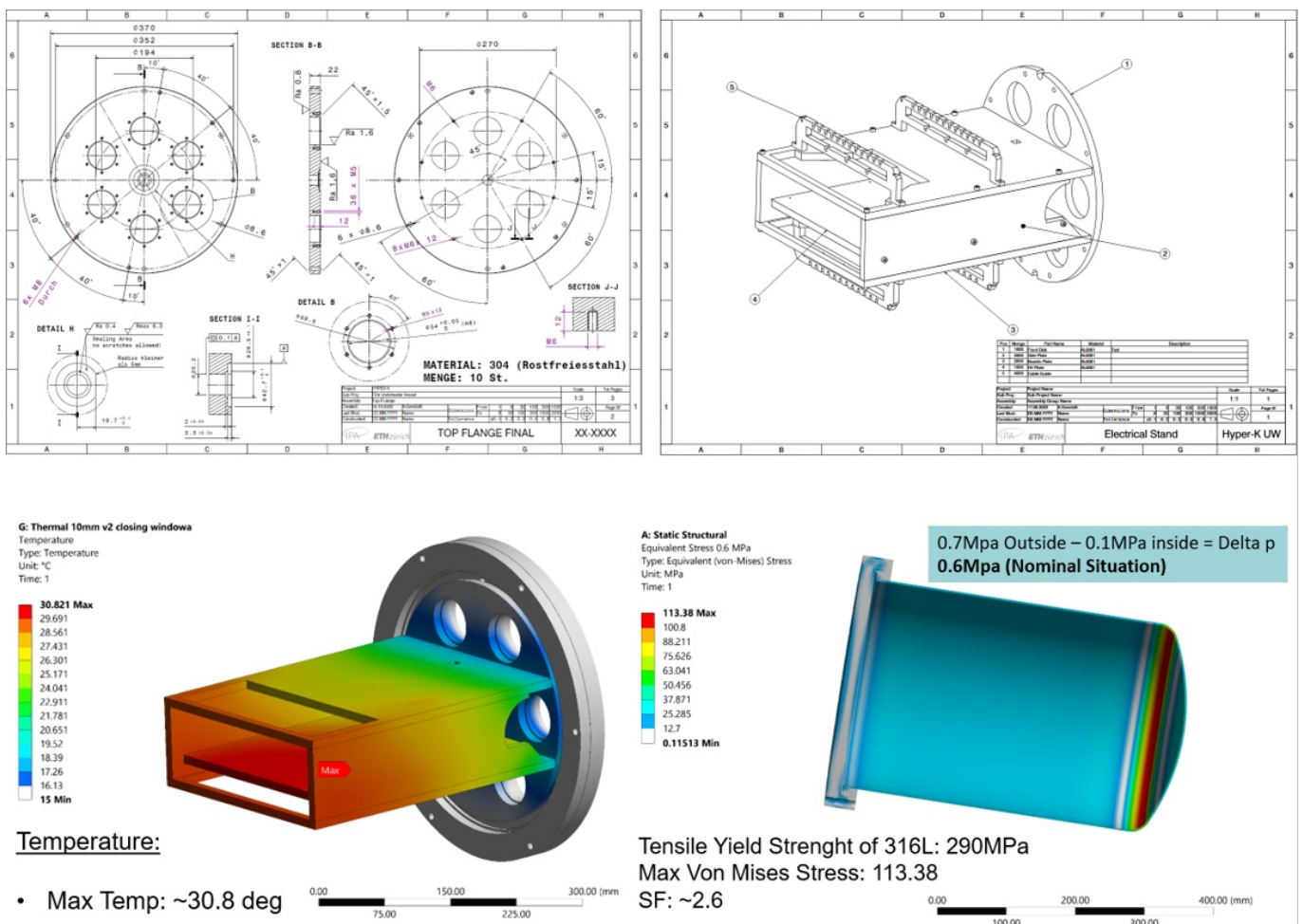


Figure 18: Top: manufacturing drawings of the Pure ID vessel design. Bottom: FEA results of the pressure applied to the vessel (bottom left) as well as of the thermal behaviour inside the vessel (bottom right).

582 As it will be shown in Fig. 24, the prototype has already been assembled with the goal of verifying,
 583 implementing and optimizing the design and the assembly procedure. A thermal test in water has been
 584 successfully performed and confirmed the results of the preliminary thermal FEA. Final pressure tests have
 585 been performed by exposing the vessel to a pressure up to 17.7 bars (about 2.5× the nominal pressure). The

586 vessel did not show any leak and no visual deformation was found.

587 At the top flange there is a total of seven water-tight feedthroughs (FT): six of them are placed on a
588 circular pattern and allow the HV and signal cables to exit the vessel and connect to the PMTs. These are
589 called PMT FTs. The remaining one is called communication FT (COM FT) and is located in the center of
590 the flange and lets the cables to connect the communication module and the power supply inside the vessel
591 with the modules outside the water.

592 The hybrid vessel has two additional 6-channel OD splitter/digitizer boards connected to the main ID
593 board by a 50 conductor ribbon cable. Two HV channels are connected to the OD splitter/digitizer boards,
594 with each HV channel powering three 3-inch PMTs. Six PMT channels will also be connected to each of the
595 OD splitter/digitizer boards. The connections to the OD PMTs is carried out through a 12-cable (RG-58)
596 FT. This will be one of the six FTs through the electronics vessel. The other five FTs will carry the remaining
597 20 ID channels. The RG-58 cable on the water side of the FT will be connected to the 3-inch PMTs.

598 3.1.7 DAQ and Slow Control

599 The Hyper-K DAQ systems will be built using the ToolDAQ framework [26]. ToolDAQ is a modular, highly
600 scalable and fault tolerant DAQ framework, which will be installed on each of the commercial computing
601 server nodes that form the DAQ system. The server nodes will be connected via commercial network switches,
602 to permit transfer of data and allow communication between elements of the system. Multiple connections
603 are used alongside dynamic service discovery to reduce the impact of hardware failure by re-routing data in
604 the event of faults. In addition, further resilience is achieved by using layers of network and networking and
605 messaging protocols within ToolDAQ.

606 Fig. 19 is a simplified diagram of the DAQ system, and shows the network layers that connect each of
607 the nodes and the front-end electronics. There are two physically separate networks. The front-end network
608 connects the Front End Electronics (FEEs) to the Readout Buffer Units via network switches. The back-
609 end network, connects the Readout Buffer Units (RBUs), Trigger Processing Units (TPUs), Event Builder
610 Units (EBUs), Brokers and other systems (e.g. archiving, monitoring and control machines). The back-end
611 network has a significant role in the processing of hit data stored in the RBUs and saving it to disk via the
612 TPUs, EBUs and Brokers.

613 Raw data from the Front-End Electronics (FEEs) is transferred via a network switch to the RBUs, where
614 it is buffered, catalogued and stored on the RBU disk and in memory for as long as possible. The flow of
615 data from the RBUs to the TPUs and EBUs is managed by a single broker. Two brokers are used to provide
616 redundancy in the system, one will always act as the primary with the other as an active backup, which
617 would be automatically used in the event of any hardware issue. Whilst the broker manages the flow of data
618 within the DAQ systems by assigning jobs/tasks to the Trigger Processing Units (TPUs) and Event Builder

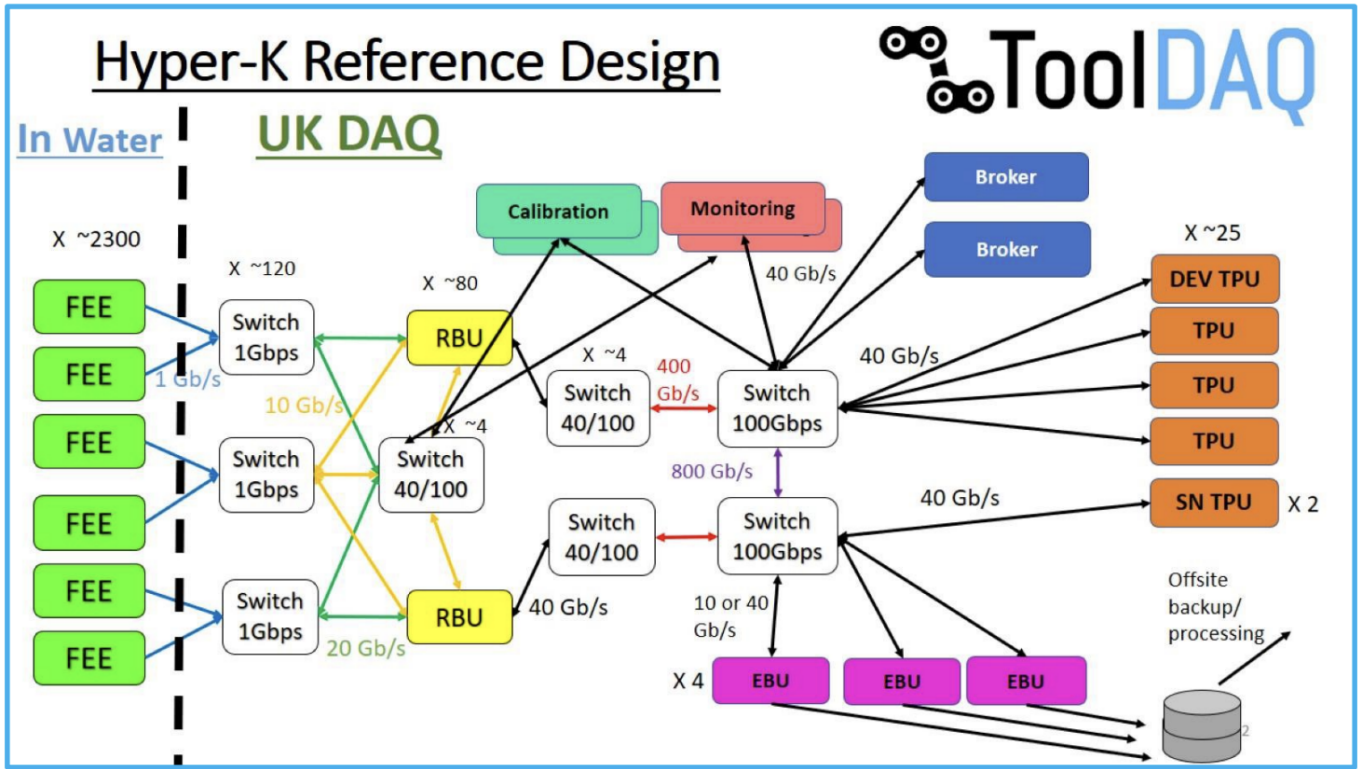


Figure 19: Diagram of the reference design for the Hyper-Kamiokande DAQ systems.

619 Units (EBUs), it does not participate in the actual transfer of data. The broker issues instructions to the
 620 TPU and EBU nodes requesting them to analyse or save data respectively and crucially, it maintains records
 621 of the results and job/task assignments. Once allocated a task, The TPU and EBU nodes request the data
 622 for their assigned jobs independently from the RBUs.

623 Incoming data is split into slices of ~ 100 ms and ~ 1 ms pieces are handed to the TPUs, where a series
 624 of trigger algorithms are applied. Decisions from the triggers are returned to the Broker, where if at least
 625 one trigger is passed, data is handed to the EBUs where it is prepared for permanent storage. Once a
 626 predetermined file size is reached, the data is archived off site, where it can be accessed for later processing
 627 and analysis.

628 For the proposed electronics tests and assembly at CERN, a small-scale version of the Hyper-K DAQ
 629 systems will be used. This will provide an ideal opportunity to test the performance and stability of the DAQ
 630 systems and the full readout of the Hyper-K data chain. In addition, a small-scale version of the monitoring
 631 and slow control system would be deployed for the assembly and testing work.

632 3.2 Ongoing activities at CERN

633 Currently two main activities are ongoing at CERN: the electronics vertical slice test (VST) and the 10-units
 634 test.

635 The VST will prove the functioning of the full electronics chain, testing all the sub-components together

636 to read a 20-inch PMTs, and verify the integration procedure.

637 The 10-unit test will verify the electronics performance in the “real” conditions. This test will be par-
638 ticularly useful to check the long-term temperature stability and the cross-talk effects when the electronics
639 boards are mounted and cabled on the mechanical stand.

640 The schedule of the ongoing tests is shown in Fig. 31 together with the overall assembly project one.

641 3.2.1 Vertical Slice Tests

642 The vertical slice test (VST) is a precious tool because it provides feedbacks to validate the final electronics
643 design. The main goals are:

- 644 • the validation of the subsystems’ compatibility, i.e. to verify that the various component interfaces are
645 correctly set;
- 646 • performance tests, i.e. study the whole system performance and compare it to the one obtained when
647 testing every single component independently and to the one obtained when the whole system is
648 enclosed in the vessel;
- 649 • optimize the integration and assembly procedure;
- 650 • the definition of the integration test protocol and mechanical tools;
- 651 • Electro-Magnetic Interference (EMI) immunity test, to define the vessel grounding scheme;
- 652 • vessel thermal profile test, i.e. study the temperature reached by the various components and the
653 definition of the cooling system plate.

654 The test will require all the elements to read and control the PMTs including the one to be installed out of
655 the water such as the set of boards in the front-end vessel, the time distribution system, the data acquisition
656 system, and the external power supplies that will provide the main power to the LV/HV modules. To make
657 it more realistic and to prepare the integration phase, also mechanical supports, water-tight connectors, and
658 feed-troughs will be used.

659 To fully simulate the analog signals to be converted, pattern generators and real PMTs will be used. The
660 last will also serve to test the HV module together with dummy loads.

661 The VST will be carried out using a sort of continuous integration procedure, on which the various
662 electronic components will be constantly updated following their development.

663 This effort has started in May 2023 when the current prototypes of the data processing board, the
664 digitizers, and the second time distribution layer have been connected together for the first time. In the time
665 prior to the boards design finalization, the bench will be used to check the interfaces and verify that all the

666 sub-systems comply with the specifications. Also firmware and software development will be carried out. In
667 parallel to the electronics design, verifications will be conducted on the mechanical part giving important
668 feedback to the mechanical design and helping to finalize the integration procedure.

669 Once the whole system is considered stable enough, four front-end units will be fully integrated in vessels
670 and tested in water using the 10-units test facility (see Sec. 3.2.2). This will represent a further step to test
671 the hardware in conditions that are as close as possible to the real one.

672 The criteria that have been established to evaluate the stability of the system are the following:

673 • DPB

- 674 – the DPB can exchange data with the DAQ;
- 675 – the DPB firmware and software can be updated over the data communication channel and the
676 fallback mechanism works in case of corrupted firmware;
- 677 – slow control data can be acquired properly.

678 • Digitizer:

- 679 – the digitizer can transfer data at nominal speed;
- 680 – charge and time resolutions are within specs;
- 681 – the firmware can be updated remotely and the fallback mechanism works properly.

682 • The LV/HV are delivered properly and the slow control is correctly exposed to the DPB.

683 • The grounding scheme has been fully tested and the electromagnetic interferences are under control,
684 including tests with long cables and PMTs (either bases only or full photodetectors).

685 • The thermal profile of the system is stable and no hot spots are present on the boards.

686 • The time distribution system can transfer clock and synchronous data to the DPB.

687 • The overall system performances do not change when the vessel is closed (to be verified with quick
688 tests due to possible thermal issues).

689 While the 4 units will be tested in water, the VST system in air will be kept operational to have a
690 reference and to help understanding any possible misbehavior on the fully integrated systems.

691 **3.2.2 10-unit tests**

692 As discussed in Sec. 3.1, the front-end electronics together with LV and HV power supply boards will be
693 placed inside the stainless steel pressurized vessel and then submerged into the water. The electronics will

694 not be accessible during the experiment lifetime. Therefore it is very crucial to have long-term reliability of
695 the system. A 10-unit test aims to identify possible failure modes of the complete system, whether related to
696 mechanical, thermal or electrical interference, or due to the setup itself, as well as to study possible ground
697 configurations. The test platform is also considered to develop and tune the slow control and the DAQ
698 system of the experiment.

699 The 10-unit test is composed of six dummy underwater units for testing the long-term stability and
700 reliability of LV and HV boards and four fully-assembled underwater units with full electronics to study the
701 integration of electronics, grounding as well as noise emissions. The dummy units include LV, HV prototypes,
702 dummy digitizers and DPB, and dummy feedthroughs. Dummy boards are designed by taking into account
703 the size of the digitizer and DPB boards, their fixing holes, the type of connectors, and the position of the
704 active components, such as FPGAs, ADC, SFPs, etc. Heat resistors placed on dummy boards are used to
705 simulate the heat dissipation of active components. The heat transferred inside the vessel will be checked
706 to study how the electronics stand can convey the heat to the water outside the vessel as well as how the
707 performance of the HV and LV modules are affected. Currently, a 40-pin flat cable is used as COM FT
708 providing 48V to the LV board and communicating with LV, HV, and dummy boards. Two dummy PMT
709 FTs are used to provide a 6 M Ω dummy load for the HV board in order to simulate the PMTs. Moreover,
710 dummy feedthroughs are also used to test the water tightness of the vessel. Fig. 20 shows one of the assembled
711 dummy units. As shown in Fig. 21, six units have been installed at CERN in Building 182 in the WA105
712 $3 \times 1 \times 1$ m³ cryostat tank filled with water, to reproduce the conditions as close as possible to the Hyper-K
713 FD.

714 The four remaining units will have all the components (HV, LV, DPB and Digitizer prototypes) and will
715 be placed underwater with the available PMT FTs and COM FT and added to the six as-yet running units.
716 The work was carried out with the help of CERN electrical technicians, in particular in the preparation of
717 cables, setting up the main power system, and providing technical support when needed.

718 The plan is to run the test for about one year to check the long-term reliability of the system.

719 **3.3 The design and production schedule of the electronics underwater units**

720 A simplified version of the Hyper-K FD electronics project schedule is shown in Fig. 22. The digitizer board
721 design will be finalised by the end of 2023 and, after the final checks and validations are performed, the mass
722 production will start in the second half of 2024. Both the HV and LV module mass production will start
723 around Fall 2023 and beginning of 2024, to be completed in the beginning of 2025. The same applies to the
724 mass production of the underwater vessels and related components.

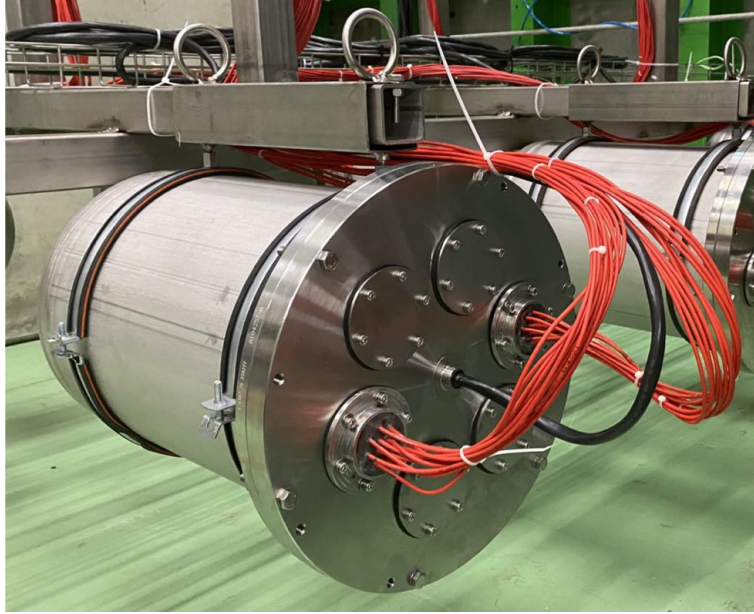


Figure 20: Fully assembled dummy unit. The black cable is used as dummy COM-FT and the red cables indicate the dummy PMT FTs.

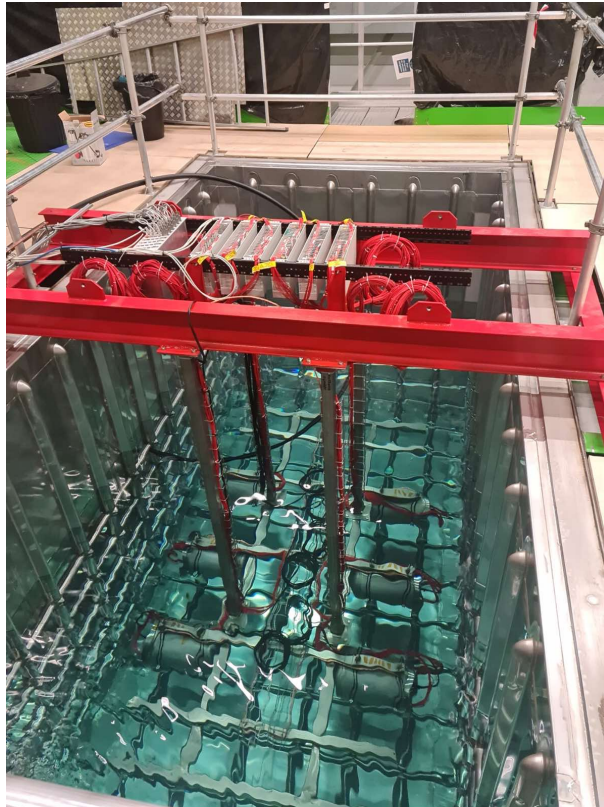


Figure 21: The 10-units set-up: the six dummy underwater units are immersed in water in the WA105 cryostat tank.

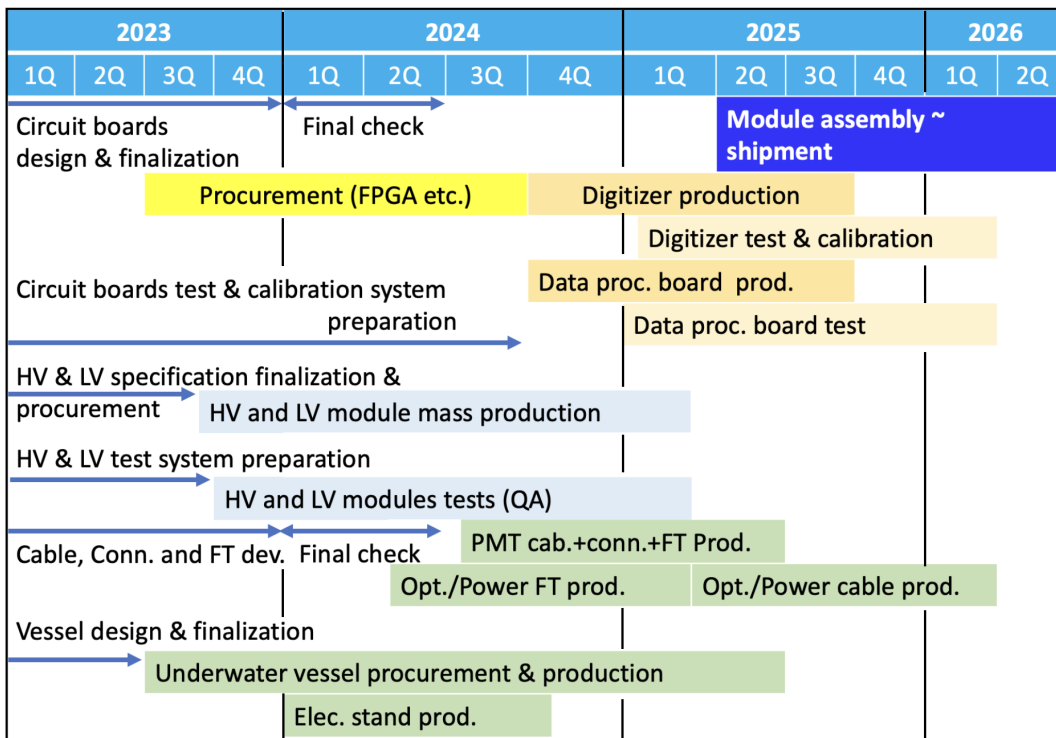


Figure 22: Hyper-K FD electronics schedule.

725 4 The Hyper-K Assembly project at CERN

726 The goal of the project is to assemble all the 900 underwater electronics units, ensuring their functioning
727 and the shipment to the Hyper-K experimental site, where they will be installed inside the FD tank in 2026.

728 More in detail, the collaboration will

- 729 • supervise the mass production of the underwater electronics unit components and coordinate the ship-
730 ment to the assembly site at CERN where they will be temporarily stored;
- 731 • assemble all the underwater units;
- 732 • ensure the functioning of the underwater units;
- 733 • ship all the underwater units to the Hyper-K experimental site in Kamioka.

734 The various activities will be shared by all the institutes involved in the project, that will also participate
735 to daily shifts to be organized in order to keep the Hyper-K target schedule.

736 The institutes involved in the underwater unit design and production will provide the support and the
737 expertise during the tests and the assembly. The collaboration organization is shown in Fig. 23. Spokepersons
738 and the technical and safety coordinators have been appointed. A contact person have been defined for each
739 underwater unit sub-component as well as for the test bench that will be used to test the functioning of all
740 the units (see Sec. 4.1.2).

741 In Tab. 4 the list of institutes involved and their commitment to the project is shown.

742 **The Hyper-K Underwater Electronics Assembly project will necessitate of space, support**
743 **for the logistic and shipment, facilities and technical expertise. Moreover, the collaboration**
744 **consists of mostly European institutes. Hence, we propose CERN SPSC to host the project**
745 **under the program of the CERN Neutrino Platform.**

746 **Fruitful discussions with the leaders of the CERN Neutrino Platform are currently ongoing.**
747 **The CERN Neutrino Platform expressed full support to host the project under its program.**

748 4.1 Planned activities

749 In this section a detailed description of the activities at CERN is given. They will consist of

- 750 • supervising the mass production of the underwater unit components;
- 751 • coordinating the shipment to the assembly site at CERN where they will be temporarily stored;
- 752 • testing the functioning of the components before the assembly;
- 753 • calibrating the digitizer;

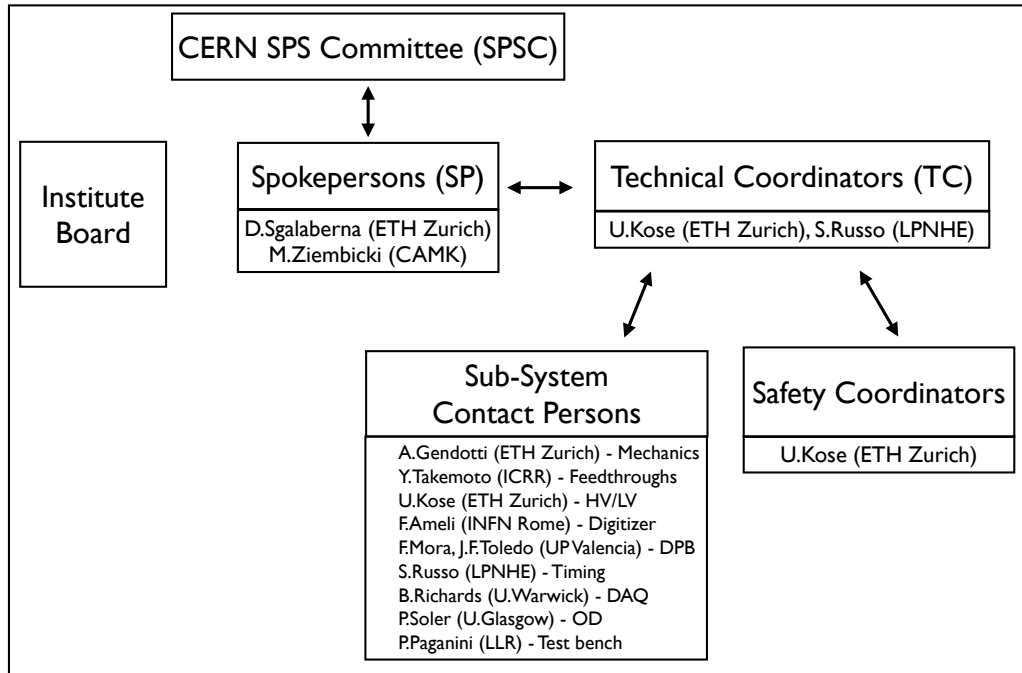


Figure 23: Organigram of the assembly project.

- 754 • assembling all the underwater units;
- 755 • testing the functioning of the assembled units in and out of water;
- 756 • performing vessel pressure tests;
- 757 • long-term tests for the system reliability;
- 758 • shipping all the units to the Hyper-K experimental site in Kamioka.

759 The following sections describe in detail the assembly and test activities.

760 4.1.1 Assembly of the underwater unit

761 The steps necessary for the underwater unit assembly have been studied and tested with a prototype to
 762 understand the potential weaknesses of the design and to optimise the assembly procedure. The main steps
 763 are shown in Fig. 24 with the following numbering: (1) assemble the DPB board on the support plate; (2)
 764 mount the HV and LV modules on the support plate and assemble the side aluminum walls; (3) assemble
 765 the HV, LV, DPB on the electronics stand, sandwiching the HV plate between the LV and DPB ones, mount
 766 the two digitiser boards and route the internal cables; (4) mount the front disk on the electronics stand; (5)
 767 mount the top flange on the electronics stand, mount the feedthroughs on the lid and insert it with the cables.

	Item	Institutes
Unit sub-components	High Voltage Low Voltage Vessels and related	ETH Zurich, U.Geneva, U.Glasgow
	Digitizer ID	INFN and U. of Naples, Padua, Pisa, Rome
	Digitizer OD	U.Glasgow
	Data Processing board ID	U.Politècnica Valencia, WUT Warsaw CAMK Warsaw, AGH Krakow, UJ Krakow
	Clock distributor	IN2P3 LPNHE, Irfu CEA Saclay, INFN and U.Rome
	Power supply (AC to DC)	ICRR Tokyo
	DAQ and Slow Control	U.Warwick, King's College of London, Lancaster University
	Feedthroughs, power and fibre cables, PMT connectors	U.Glasgow, ICRR Tokyo, U.Tokyo
Assembly related	Test bench	IN2P3 LLR
	Pressurized tank	ETH Zurich
	Assembly activities	All institutes

Table 4: List of institutes involved in the Hyper-K FD underwater electronics and related activity commitment.

768 This step is the most delicate in the assembly process because mistakes could result in the penetration of
769 water inside the vessel. Thus, qualified technicians will be required; (6) connect the power cable at the front
770 side; (7) connect the HV, optical and signal cables to the respective boards; (8) check the cable routing and
771 add the side aluminum plates to complete the electronics stand; (9) insert the electronics stand inside the
772 aluminum vessel and close it.

773 A stand is needed to support the mechanical vessel during the assembly and mount the boards inside
774 and route the cables in an easy way. An initial design is shown in Fig. 25. First the top flange of the
775 vessel is installed on the frame which will have wheels to facilitate its transport from the storage area to the
776 assembly room. Supports are needed for the ~ 3 m long cables that connect the electronics to the PMT
777 cables. Moreover, it shall provide the possibility to rotate the vessel by 180° . The support stand has to be
778 designed, purchased and produced. A minimum of four support stands is foreseen.

779 A total of eight technicians full time are planned, two working together on the same vessel, for a total of
780 four assembly stands. Such approach will allow to keep the necessary pace during the assembly to meet the
781 time schedule requirements, described more in detail in Sec. 4.3.1.

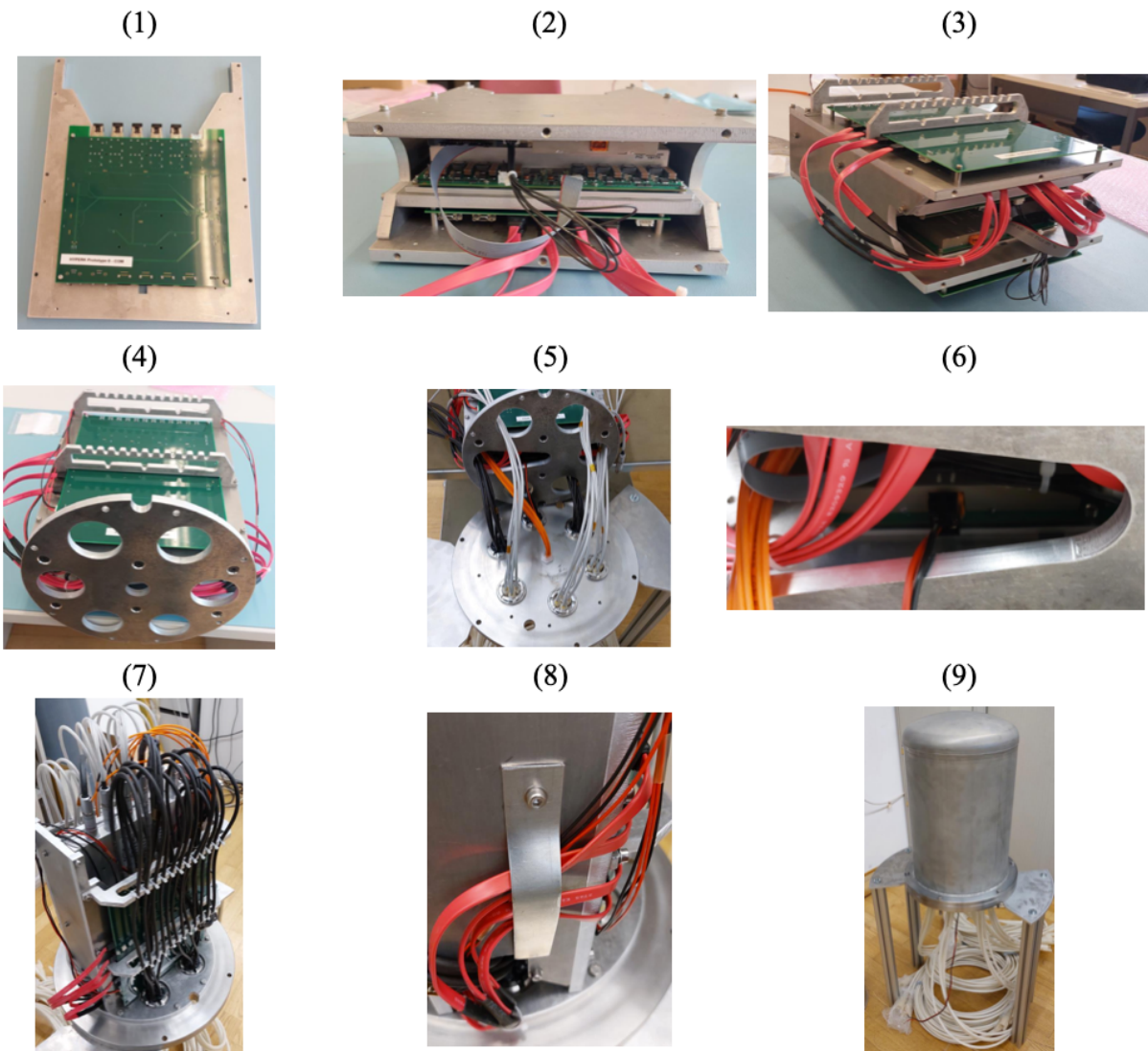


Figure 24: Summary of the steps necessary for the assembly of an underwater electronics unit.

782 4.1.2 Electronics tests

783 During the whole integration process, tests will be performed to verify the various steps of the assembly
 784 procedure. The full test set can be divided into pre-assembly and during-assembly.

785 **Pre-assembly** Before starting the integration, the digitizer board will be carefully characterized injecting
 786 precisely controlled analog signals and analyzing the conversion results. This procedure will be carried out at
 787 different temperatures and by swiping all the converter dynamic range. This work represents a fundamental
 788 step that will facilitate the data analysis once the full detector will be operational.

789 **During-assembly** The assembly process will be controlled with a series of tests that will verify the various
 790 steps of the procedure and, to make the verification process effective and efficient, an automated test bench
 791 will be developed. It will be composed of a subset of the DAQ and time distribution system, dummy loads



Figure 25: Conceptual design of the support stand for the fixation of the mechanical vessel and the installation of the boards and cables inside (left), photo of the simple support used for testing the assembly steps (middle) and conceptual model of the pressurized tank (right).

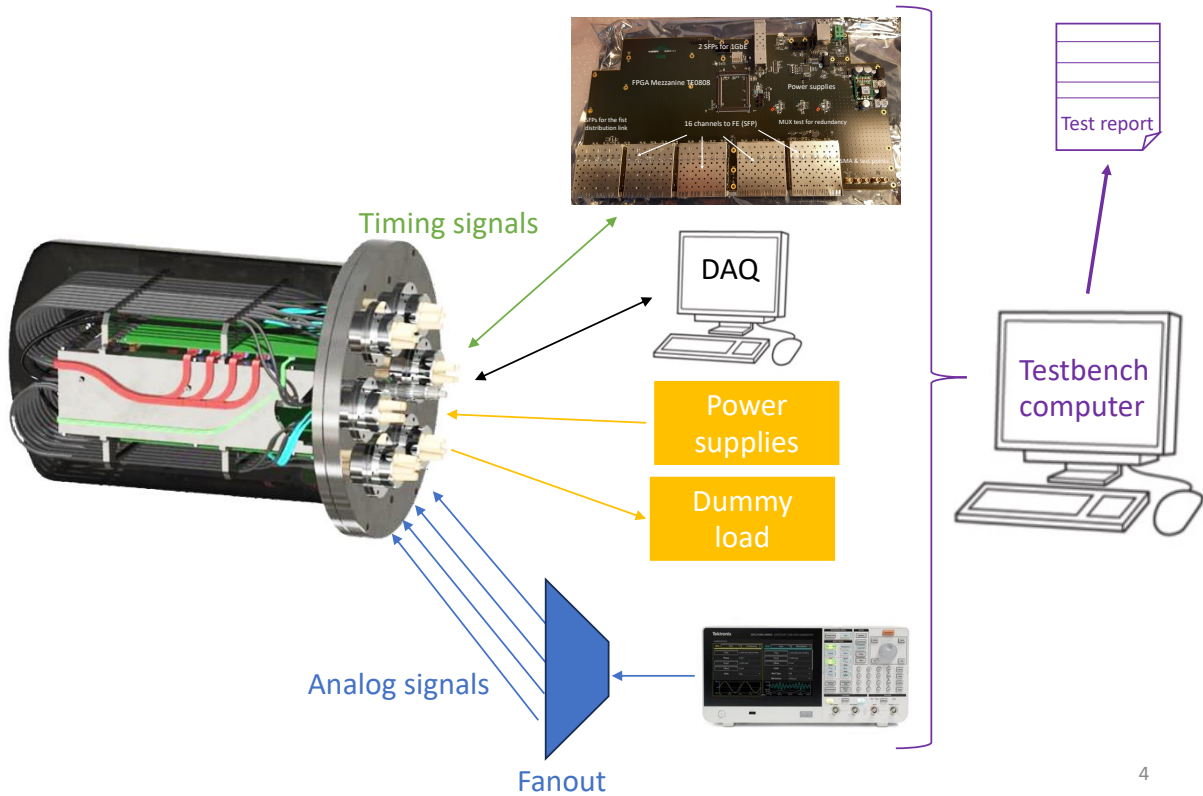
792 to simulate the PMT connection to the high voltage system, a Tektronix pulse generator (a wide range of
 793 arbitrary function generator is available, AFG31252 for example) with an amplifier and signal switching
 794 boards with fan-out, provided by the Korean Hyper-K group including Kyungpook National University,
 795 Center for Precision Neutrino Research, Chonnam National University, and Seoul National University, to
 796 inject well known signals from a single source into the digitizers and a power supply to provide current to
 797 the front end module under test. A block scheme of the test stand is reported in Fig. 26.

798 The relation of the timing of the analog signal and the reference clock is independently recorded. This
 799 feature will allow not only to verify the conversion process but also to check that the main clock is correctly
 800 distributed to the boards. The converted data will be acquired using the data acquisition system and
 801 automatically analyzed. The results will be compared to a benchmark to provide a pass/fail result. The
 802 entire procedure will be carried out by means of a set of software scripts to reduce human interventions and
 803 possible errors.

804 Testing the electronics assembled on the stand together with the flange and the water-tight connectors
 805 and feed-troughs will allow to check the entire system and the various interfaces. A test report, that will
 806 contain the board serial numbers as well as the test result, will be produced and stored in a database.

807 4.1.3 Pressurized tests

808 Once the assembly of an underwater electronics unit is completed, a custom-made setup will be used to fully
 809 test both its mechanics and the electronics performance in the same conditions (pressure and temperature) as
 810 inside the Hyper-K FD tank filled with water. Such test shall be performed under pressure, also to validate



4

Figure 26: A block scheme of the electronics test stand that will be used during the installation process. In the center the front end board mounted on the stand and the flange with the connectors. On the right side of the picture the equipment to perform the test are presented.

811 the water-tightness at the pressure to which it will be exposed in the FD tank.

812 The conceptual model of the pressurized tank is shown in Fig. 25. Such test has yet to be fully studied.
 813 The pressurized tank has to be engineered, designed, studied with finite-element analysis (FEA) and, even-
 814 tually, approved by the CERN Occupational Health and Safety and Environmental Protection Unit (HSE),
 815 before being purchased. A mechanical engineer will be necessary for this task. The design shall be optimized
 816 also for an easy opening and closure of the underwater vessel and shall ensure an easy and safe routing of
 817 the PMT cables from the vessel feedthroughs to outside the pressurised tank setup.

818 4.1.4 Long-term tests

819 As discussed in Sec. 3.2.2, the current 10-unit test will last until the end of 2024 verifying that all components
 820 of the underwater vessels can run reliably under extreme conditions. Additional tests are planned to be
 821 performed until Summer 2026. We are planning the delivery of the electronic boards in batches. A sub-
 822 sample of the unit components will be taken from each delivery batch and will be used to assemble 10
 823 additional underwater electronics units. A 100 to 150 m long COM FT cable with two wire cables and
 824 optical fibers will allow testing voltage drop on the cable as well as to identify the presence of noise picked

825 up from the environment. The cables coming out of the PMT FTs will be connected to 20 m long PMT
826 cables, ensuring a watertight connection, and then soldered into 6 M Ω dummy load to simulate the PMT.

827 The test would be carried out by using the same infrastructure as that of the ongoing 10-unit test, i.e.
828 the WA-105 cryostat tank in building 182 at CERN, as shown in Fig. 21. A test stand, analogous to the
829 one used for testing the units during the assembly, will be used to control and monitor the whole system
830 (Sec. 4.1.2).

831 4.2 Assembly project definition

832 The collaboration has identified the main project items, which include: the space for the storage of the
833 900 unit components, for the test and the assembly activities as well as for the shipment of the assembled
834 units (see Sec. 4.2.1); the long-term tests, described in Sec. 4.1.4, to be carried out in the WA-105 cryostat
835 in building 182 (see Sec. 4.2.2); qualified personnel (see Sec. 4.2.3), such as one mechanical engineer for the
836 design of the test and assembly tools and equipment (see Sec. 4.1.1 and Sec. 4.1.3). Moreover, technicians
837 will be needed to take on the more delicate tasks during the underwater unit assembly steps.

838 4.2.1 Space for storage and activities

839 The activities for the underwater unit can be divided in three macro areas: the storage area, to host the
840 components just delivered from the supplier to the assembly site; the assembly and testing area; the shipping
841 area. The estimated total amount of space needed, as shown in Fig. 27, is about about 850 m², of which
842 300 m² are for the tests and the assembly. For logistic reasons a close collocation of the various areas would be
843 preferable. **Such first estimate is currently under study. Further optimisations, like increasing**
844 **the pipelining of the underwater components, are ongoing in coordination with the CERN**
845 **Neutrino Platform.**

846 Storage area

847 A big fraction of the area will be taken by the mechanical vessels, that could be stored outside still
848 in the pallets used for the shipment. One pallet will contain 6 units, for a total approximate surface of
849 120 cm \times 80 cm. As it would be worth avoiding the stacking of different pallets, it may be not trivial to
850 further reduce the size of this area. Optimisation could rely on a higher delivery rate with smaller batches.
851 For the electronics stands, boxes containing 10 units, for a total volume of 80 cm \times 60 cm \times 50 cm are
852 estimated. They shall be stored inside and with the possibility of stacking boxes. Overall, about 150 units
853 per month are expected. Concerning the PMT FTs, boxes containing 4 units, for a total volume of about
854 55 cm \times 45 cm \times 25 cm, can be stored inside. Both the LV and the HV boards, will be delivered in batches
855 of 5 units contained in a box of about 60cm \times 40cm \times 50cm. They shall be stored inside with the possibility

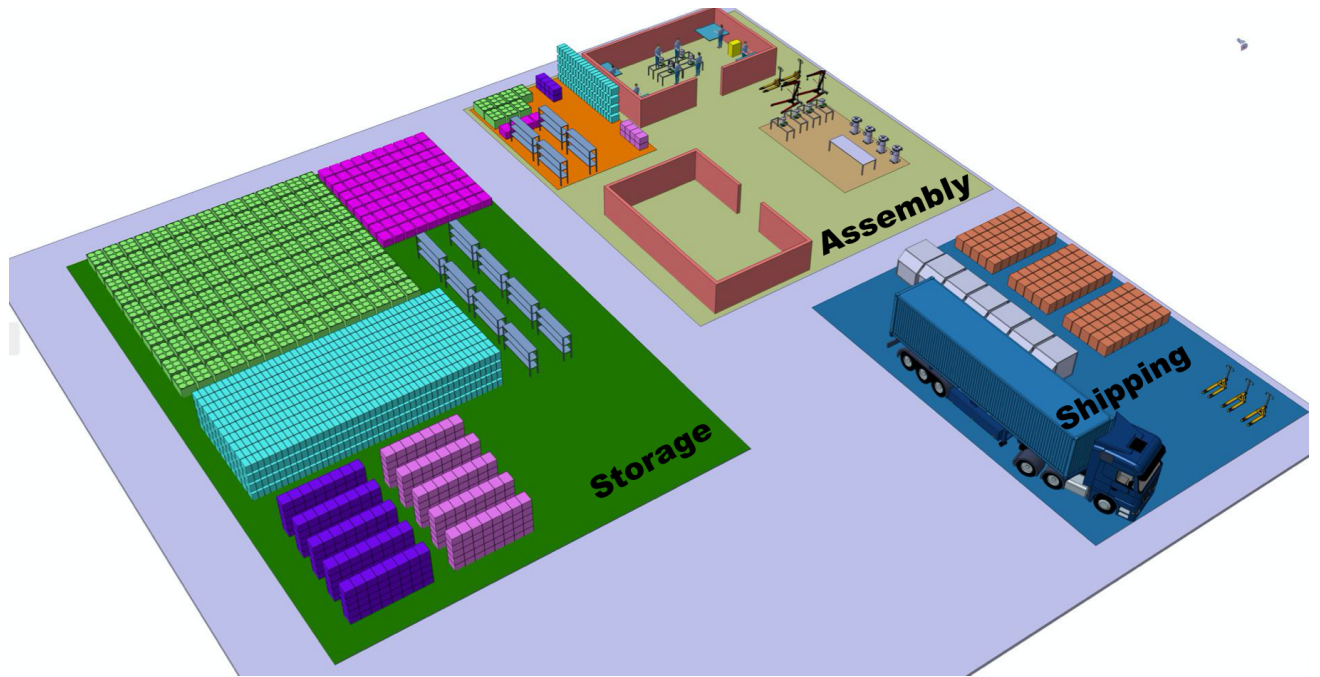


Figure 27: Estimated needed spaces for the various project activities: storage, assembly and tests, shipping.

856 of stacking up to 5 boxes in order to reduce the full area. Given the very similar dimension between the LV
 857 and HV modules, two areas of the same extension will be needed. The remaining components, i.e. COM
 858 FTs, digitizer boards, DPB boards, bolts and nuts, will need relatively small boxes and will take a small
 859 fraction of the total space, also because they can be stored in dedicated shelves.

860 The total area shall also facilitate the possibility of moving components from different places, also using
 861 movable cranes and a pallet transporter. Overall, a total area of approximately 250 m² has been estimated.
 862 It accounts for about 30% of the full capacity needed for all the 900 units, in order to provide enough buffer
 863 space in case the assembly has to stop but the delivery of the components from the supplier companies shall
 864 continue. The estimated storage area can be found in Fig. 28.

865 **Assembly and Test area**

866 This area shall be compatible with the planned daily routine needed for the assembly and the test of
 867 the underwater units. The assembly area will be divided into four main areas, for a total of approximately
 868 300 m². It includes a weekly storage area to contain up to approximately 40 vessels. Further optimisation
 869 could be achieved if, for example, only daily vessel storage is planned. The assembly area will have to include
 870 at least 4 assembly stations where 8 people will work simultaneously. Depending on the space available, a
 871 tent for environment protection may be used. An area will be dedicated to the integrated electronics and
 872 pressurized tests, while another area might be needed if additional tests will have to be included or, for
 873 example, if offices will be needed.

874 In each assembly station the following daily routine is foreseen:

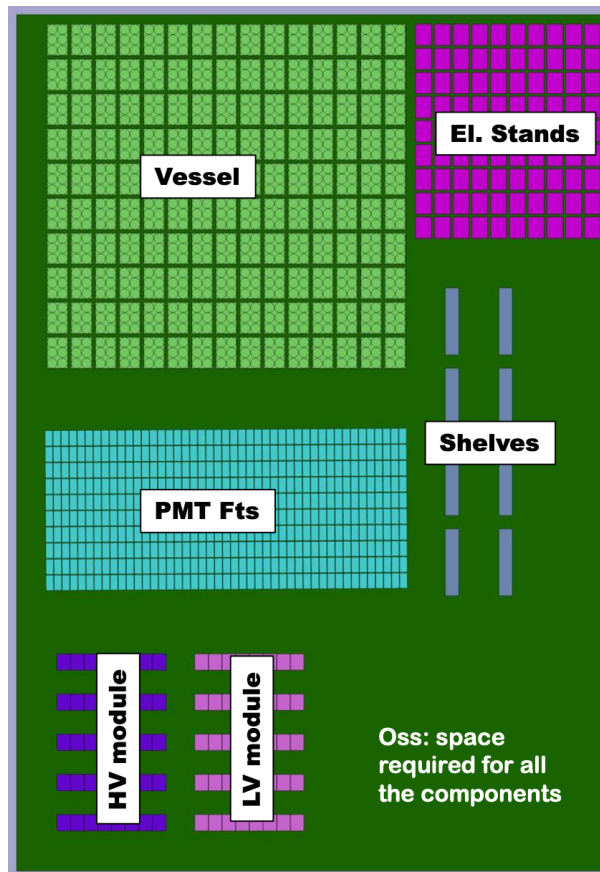


Figure 28: Estimated space needed for the storage of the underwater unit components.

- 875 • prepare the weekly/daily storage;
- 876 • prepare the assembly stations;
- 877 • start the assembly of the underwater unit with the electronics stand and the top flange;
- 878 • perform the first integrated system tests;
- 879 • close the vessel once the electronics units are installed inside;
- 880 • perform the final integrated system test in pressurized water to fake the conditions to which the
- 881 underwater unit will be subjected once in the Hyper-K FD tank;
- 882 • place the assembled and validated underwater unit in the shipping box;
- 883 • eventually, the shipping box will be moved to the shipping area.

884 The estimated assembly and test area is shown in Fig. 29.

885 Shipping area

886 The shipping area will allow to store the boxes containing the underwater units ready to be shipped to

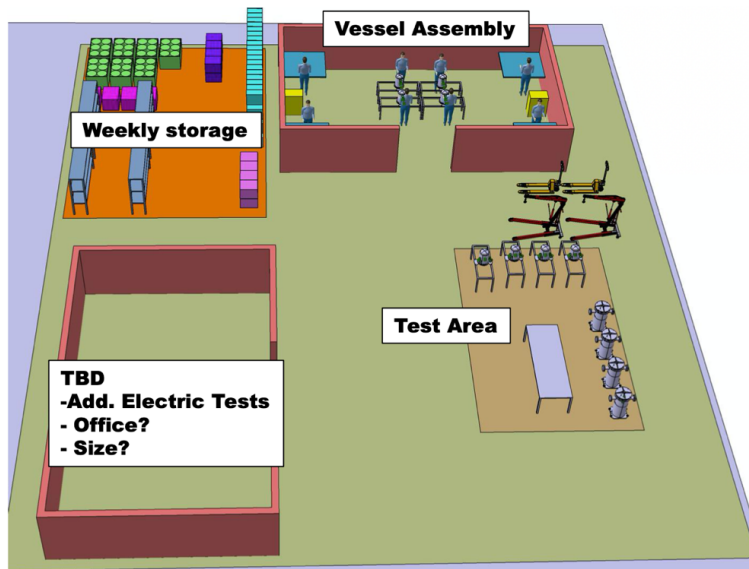


Figure 29: Estimated area of the area dedicated to the assembly and the test of the underwater units.

887 Japan. Preliminary estimates account for a weekly quantity of 20 to 40 boxes to be stored in this area. We
 888 are considering stacking of multiple boxes in order to reduce the size of the area.

889 A loading area shall include the space for the containers ready for shipment, the access for trucks to pick
 890 up the containers, and free space for workers to load and prepare the boxes.

891 Eventually, a buffer area is needed to prevent from piling up with multiple boxes and from filling the
 892 loading area, in case the shipping has to stop while the assembly activities continue. Ideally, the ship-
 893 ping/loading area should be relatively close to the assembly area to facilitate the movement of the boxes
 894 with the assembled units from one site to the other.

895 A total area of approximately 300 m² is currently considered. A sketch of the estimated area can be
 896 found in Fig. 30.

897 4.2.2 WA105 facility for long-term tests

898 As described in Sec. 4.1.4, we plan to perform long-term tests with some fully-assembled underwater units.
 899 The test would be carried out by using the same infrastructure as that of the ongoing 10-unit test, i.e. the
 900 WA-105 cryostat in building 182 at CERN, as shown in Fig. 21.

901 4.2.3 Person power and technical personnel

902 Several of the project tasks can be carried out by the members of the Hyper-K collaboration:

- 903 • testing the electronics with the available test benches or moving components from one site to the other.
- 904 Standard tasks will be taken by “shifters”, i.e. members of the Hyper-K collaboration with no particular
- 905 roles in the project or technical qualifications;

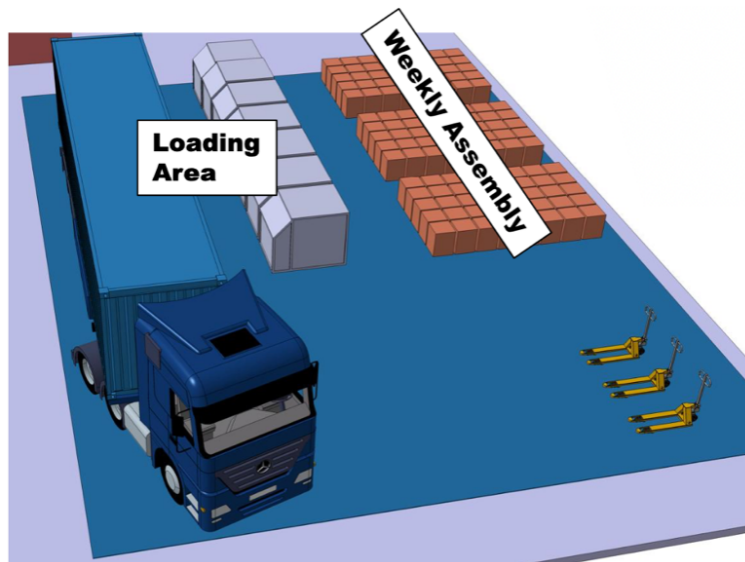


Figure 30: Estimated area dedicated to the storage of the assembled underwater units and the shipment to the Hyper-K site in Japan.

- 906 • supervise the logistic, i.e. check the arrival of the equipment, the workflow, and keep the contact with
907 CERN staff (shipment and safety). This role will be taken by the project technical coordinators present
908 on site;
- 909 • supervise each sub-system of the underwater unit. This task will be taken by the contact persons listed
910 in Fig. 23;
- 911 • overall supervision of the project. It will be ensured by the spokespersons, with the support of the
912 technical coordinators.

913 However, the project will also necessitate dedicated person power to carry out particular tasks:

- 914 • 8 qualified technicians to take care of the main assembly work of the underwater units (8 hours per
915 day, 5 days per week for 45 weeks, for a total of 14'400 hours). The goal is to complete the assembly
916 of at least 4 vessels per day. Tasks like the installation of the feedthrough assemblies in the vessel are
917 critical and delicate, hence they cannot be taken by the shifters. The technicians would be hired from
918 the CERN Field Support Units (FSU) and will be budgeted within the Hyper-K funding scheme;
- 919 • External company for the preparation of the boxes for transportation. The work will have to be carried
920 out on-site (e.g. filling the shipping containers). The outside of the vessel should be sufficiently clean
921 to not degrade the FD water quality, for instance by placing it in a vinyl bag, like the one used for
922 20-inch PMT (still, before the installation in the FD the vessels and the cables will be cleaned);
- 923 • support from CERN staff for shipping, i.e. for usage of crane, forklift, etc. 3 persons, 2 days per week
924 for 45 weeks for a total of about 2'160 hours are considered a reasonable preliminary estimate;

- 925 • A mechanical engineer in charge of the design and the production of the custom-made equipment
926 (approximately 1 month of full-time work), that would be hired from the CERN FSU and budgeted
927 within the Hyper-K funding scheme.

928 4.2.4 Computing

929 In addition to the items described above, it will be useful to have dedicated computing resources to store
930 the data collected during the electronics tests. About 100 TB should be sufficient for the entire dataset.

931 4.3 Project milestones, time schedule and costs

932 4.3.1 Project schedule

933 The inputs to the project organization described in the previous section are based on realistic assumptions
934 and, at the same time, fulfill the requirements of the overall Hyper-K schedule.

935 The schedule of the assembly project is shown in Fig. 31. The mass production of the sub-system
936 components will start in the second half of 2023 and will end in Fall 2025. The production will be done in
937 different batches that will be immediately shipped to CERN once ready. The batch sizes and delivery rate
938 is currently under definition in order to optimise the space that can be provided for the project.

939 The currently ongoing activities at CERN, i.e. the vertical slice tests (VST) and the 10-units tests, have
940 started recently. While they both will provide important results in Fall 2023, they will run for up to 1 year in
941 order to check the stability of the system, both in and out of water, and validate the ageing of the underwater
942 unit components.

943 The preparation for the project has started and the number of activities will increase, in particular
944 starting from 2024 when the project plan will have to be finalised and the engineering work for the assembly
945 stand, pressurised tank, electronics test bench will be ongoing.

946 The overall project will take about 2 years. It will mostly take place in 2025, starting from system tests,
947 i.e. the calibration of the digitizer boards, followed by the actual assembly of the vessels. The shipment of
948 the 900 underwater unit components will be done in different batches. The last batch is expected to arrive
949 at the Hyper-K site in Kamioka by the end of August 2026.

950 4.3.2 Project costs

951 A preliminary cost estimate of the overall project includes a complete set of tools and commercial equipment
952 for the assembly activities. The main items are related to the cleaning of screws and metallic parts before
953 the assembly. Chemical products will be required and proper storage will have to be ensured. Also ultrasonic
954 bath can be used. Shelves, tables, cupboard, etc. will be needed for the storage of small components as well
955 as movable cranes and pallet transporters to facilitate the transport of the vessels.

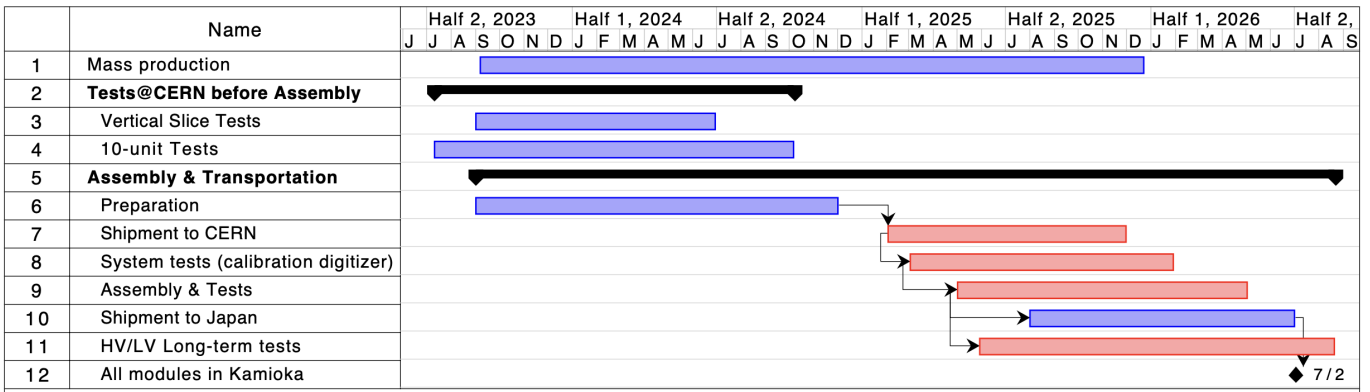


Figure 31: Simplified Gantt chart of the Hyper-K Assembly project.

956 Four pressurised tanks (one for each assembly stand) plus spares for testing the integrated underwater
 957 unit in pressurised water will have to be produced, after the custom design has been completed and validated.
 958 Four supports stands, one for each assembly station, (plus spares) for vessel assembly have to be procured.

959 Electronics test benches for the calibration of the digitizer boards and the tests of the underwater units
 960 will be needed as well.

961 The cost of the person power has been estimated. It does not include the cost for “shifters”, which will
 962 be accounted for independently by each institute. Instead, one mechanical engineer (part-time), technicians
 963 for the underwater unit assembly (both from CERN FSU) and personnel for the shipment (CERN Staff) are
 964 taken into account. A more detailed description of the person power can be found in Sec. 4.2.3.

965 Finally, a preliminary estimate of the shipment cost has been done accounting for the procurement of the
 966 shipment boxes, the in-loco packaging at CERN by the shipment company, the actual shipment from CERN
 967 to Kamioka in Japan.

968 A preliminary total cost of about 2,400 kCHF has been estimated. It includes a 30% cost contingency.
 969 Cost optimisation is ongoing and updates are expected by the time of the submission of the final proposal
 970 to the SPSC. **The Hyper-K collaboration will cover the full cost of the project, including the**
 971 **additional qualified personnel. No funding is requested to CERN.**

972 5 Conclusions and Outlook

973 The Hyper-K long-baseline neutrino experiment will search for leptonic CP violation in long-baseline neutrino
974 flavor oscillations with a realistic potential of discovery within 3 to 10 years after the start of the data taking.
975 It will measure the CP violating phase with a resolution better than 23° depending on its value and define
976 the neutrino mass ordering with a significance better than four standard deviations by combining data
977 from accelerator and atmospheric neutrinos. Beside the accelerator neutrino physics, Hyper-K will achieve
978 unprecedented sensitivities to the detection of proton decays as well as supernova and astrophysical neutrinos.

979 The Hyper-K experiment has now entered its construction phase and will start collecting accelerator and
980 atmospheric neutrino data in 2027. An essential contribution is given by European institutes, in particular
981 to the far detector underwater electronics system, that will allow to operate the about 23,600 PMTs, of
982 which 20,000 20-inch PMTs of the inner detector and 3,600 3-inch PMTs of the outer detector. Each of
983 about 900 underwater electronics units comprises a module that provides the high voltage to the PMTs, two
984 boards that digitize the analogue signal received from the PMTs, a data signal processing board, and a low
985 voltage module that provides power to all the modules within the vessel. The digitized signal is sent to the
986 on-surface DAQ system via up to 150 m long electro-optical cables used for both data and power. All the
987 components are contained in a stainless steel vessel that will be installed underwater in the far detector tank
988 and exposed to pressures up to 7 bars. The PMT signal, power and optical cables reach the sub-system
989 modules inside the vessel through water-tight feedthroughs.

990 With this Letter of Intent we propose to base the test and the assembly of the 900 underwater electronics
991 units at the CERN Neutrino Platform. We need to collect the sub-system components, calibrate the digitizer
992 boards, assemble the underwater electronics units, test them in water under pressure and ship them to the
993 far detector site in Kamioka. Such project is a common effort lead by the European institutes involved in
994 Hyper-Kamiokande, that would have easy access to the experimental facilities at CERN. We will need space
995 to store the sub-system components upon their arrival at CERN, assemble and test them and store the
996 assembled vessels before the shipment to Japan. Technical expertise (mechanical engineer and technicians)
997 and support for the shipment will be needed. CERN with its Neutrino Platform has been identified as the
998 ideal framework to carry out such project. After a preparatory phase, the test and the assembly activities
999 will start in early 2025 and will last for about 1.5 years. The WA105 cryostat tank, being used for the
1000 10-units test, would be needed to perform additional long-term tests with sub-system components from
1001 different batches for the whole duration of the project. The project will be fully funded by the Hyper-K
1002 collaboration, including the technical personnel. A preliminary project cost estimate is also provided in this
1003 Letter of Intent.

1004 Full support has been expressed by the leaders of the Neutrino Platform to host the project under its
1005 program. Currently, discussions are ongoing in order to optimise the implementation of the project, like the

1006 space required.

1007 **6 Acknowledgements**

1008 We thank Francesco Lanni and Filippo Resnati, respectively the head and the technical coordinator of the
1009 CERN Neutrino Platform, for the very fruitful discussions and their support to the project.

1010 References

- 1011 [1] Y. Fukuda et al. Evidence for oscillation of atmospheric neutrinos. *Phys. Rev. Lett.*, 81:1562–1567,
1012 1998.
- 1013 [2] Q. R. Ahmad et al. Measurement of the rate of $\nu_e + d \rightarrow p + p + e^-$ interactions produced by ^8B solar
1014 neutrinos at the Sudbury Neutrino Observatory. *Phys. Rev. Lett.*, 87:071301, 2001.
- 1015 [3] Q.R. Ahmad et al. Direct evidence for neutrino flavor transformation from neutral current interactions
1016 in the Sudbury Neutrino Observatory. *Phys. Rev. Lett.*, 89:011301, 2002.
- 1017 [4] K. Eguchi et al. First results from KamLAND: Evidence for reactor anti-neutrino disappearance. *Phys.*
1018 *Rev. Lett.*, 90:021802, 2003.
- 1019 [5] M.H. Ahn et al. Measurement of Neutrino Oscillation by the K2K Experiment. *Phys. Rev. D*, 74:072003,
1020 2006.
- 1021 [6] M. Tanabashi et al. Review of Particle Physics. *Phys. Rev. D*, 98(3):030001, 2018.
- 1022 [7] K. Abe et al. Indication of Electron Neutrino Appearance from an Accelerator-produced Off-axis Muon
1023 Neutrino Beam. *Phys. Rev. Lett.*, 107:041801, 2011.
- 1024 [8] Y.Ajima et al. Tokai-to-Kamioka (T2K) Long Baseline Neutrino Oscillation Experiment Proposal.
1025 http://j-parc.jp/researcher/Hadron/en/pac_0606/pdf/p11-Nishikawa.pdf.
- 1026 [9] K. Abe et al. The T2K Experiment. *Nucl. Instrum. Meth. A*, 659:106–135, 2011.
- 1027 [10] F.P. An et al. Observation of electron-antineutrino disappearance at Daya Bay. *Phys. Rev. Lett.*,
1028 108:171803, 2012.
- 1029 [11] M. A. Acero et al. Improved measurement of neutrino oscillation parameters by the NOvA experiment.
1030 *Phys. Rev. D*, 106(3):032004, 2022.
- 1031 [12] Fengpeng An et al. Neutrino Physics with JUNO. *J. Phys. G*, 43(3):030401, 2016.
- 1032 [13] B. Abi et al. Long-baseline neutrino oscillation physics potential of the DUNE experiment. 6 2020.
- 1033 [14] S. Pascoli, S.T. Petcov, and Antonio Riotto. Connecting low energy leptonic CP-violation to leptogenesis.
1034 *Phys. Rev. D*, 75:083511, 2007.
- 1035 [15] K. Abe et al. Constraint on the matter–antimatter symmetry-violating phase in neutrino oscillations.
1036 *Nature*, 580(7803):339–344, 2020. [Erratum: *Nature* 583, E16 (2020)].

- 1037 [16] K. Abe et al. Improved constraints on neutrino mixing from the T2K experiment with 3.13×10^{21}
1038 protons on target. *Phys. Rev. D*, 103(11):112008, 2021.
- 1039 [17] K. Abe et al. The Hyper-Kamiokande Experiment - Snowmass LOI. In *2021 Snowmass Summer Study*,
1040 9 2020.
- 1041 [18] K. Abe et al. Hyper-Kamiokande Design Report. 5 2018.
- 1042 [19] K. Abe et al. T2K ND280 Upgrade - Technical Design Report. 1 2019.
- 1043 [20] C. Bronner, Y. Nishimura, J. Xia, and T. Tashiro. Development and performance of the 20" PMT for
1044 Hyper-Kamiokande. *J. Phys. Conf. Ser.*, 1468(1):012237, 2020.
- 1045 [21] S. Bhadra et al. Letter of Intent to Construct a nuPRISM Detector in the J-PARC Neutrino Beamline.
1046 12 2014.
- 1047 [22] M. Barbi et al. Proposal for A Water Cherenkov Test Beam Experiment for Hyper-Kamiokande and
1048 Future Large-scale Water-based Detectors. Technical report, CERN, Geneva, 2020.
- 1049 [23] Megan Friend. Long-Baseline Neutrino Oscillation Physics Sensitivities of the Hyper-Kamiokande Ex-
1050 periment (NuFact 2022). <https://indico.fnal.gov/event/53004/contributions/244613/>. (NuFact
1051 2022).
- 1052 [24] K. Abe et al. Supernova Model Discrimination with Hyper-Kamiokande. *Astrophys. J.*, 916(1):15, 2021.
- 1053 [25] Michael Smy. Hyper-Kamiokande (NuFact 2022). [https://indico.fnal.gov/event/53004/
1054 contributions/242342/](https://indico.fnal.gov/event/53004/contributions/242342/). (NuFact 2022).
- 1055 [26] Benjamin Richards. ToolDAQ framework v2.1.1. <https://doi.org/10.5281/zenodo.1482767>, Novem-
1056 ber 2018.